

SCHOOL OF SCIENCE

Department of Industrial Chemistry “Toso Montanari”

Second cycle degree in

Low Carbon Technologies and Sustainable Chemistry

Classe LM-71 - Scienze e Tecnologie della Chimica Industriale

Alcohol-soluble heteroalkylthiophene derivatives:
inside the role of cathode interlayers for green
energy production

Experimental degree thesis

CANDIDATE

Cecilia Iuliitti

SUPERVISOR

Prof.ssa Elisabetta Salatelli

CO-SUPERVISOR

Dott.ssa Martina Marinelli

Prof. Massimiliano Lanzi

Abstract

The inorganic photovoltaic technology currently available on the market presents high production, purchase and installation costs, thus leading the research to focus on the development of alternative semiconductor materials, such as π -conjugated polymers. However, although the advantages of these polymers are several, they are often soluble in toxic and harmful solvents with a high environmental impact. Consequently, the development of water/alcohol-soluble conjugated polymers (WSCPs) has become the subject of extensive study, as they combine excellent optical properties with solubility in “green” solvents.

This work is therefore focused on the synthesis of two different class of thiophene-based copolymers, both containing different content of oxygen directly connected to the ring. Specifically, dye-sensitized (**P1a-TPP** and **P2a-TPP**) and push-pull (**P1b-Bz** and **P2b-Bz**) copolymers were synthesized by oxidative coupling with iron trichloride and Suzuki cross-coupling reaction, respectively. Then, by post-functionalization approach with tributyl phosphine, ionic alcohol-soluble polymers were prepared. All these materials were thoroughly characterized by means of spectroscopic techniques and subsequently tested as cathode interlayers, in halogen-free photovoltaic organic solar cells of BHJ configuration.

Table of Content

INTRODUCTION.....	1
1. FOREWORD.....	3
2.CONJUGATED POLYMERS	4
2.1 Overview.....	4
2.2 Conductivity and charge transport.....	5
2.3 Doping	6
3.THIOPHENE-BASED DERIVATIVES	8
3.1 Structures and characteristics	8
3.2 Optical properties.....	9
3.3 Synthesis of P3ATs.....	11
3.3.1 Oxidative polymerization with FeCl ₃	11
3.3.2 Suzuki cross-coupling polymerization	12
4. APPLICATION OF ICPS.....	14
4.1 Organic Photovoltaic Cells (OPV).....	14
4.1.1 Solar energy.....	14
4.1.2 Mechanism of photogeneration	15
4.1.3 Acceptor-donor materials.....	17
4.1.4 BHJ architecture.....	19
5. INTERLAYER MATERIAL	22
RESULTS AND DISCUSSION	24

1. AIM OF THE WORK	26
2. SYNTHESIS	28
2.1 Preparation of the monomers	29
2.2 Preparation of precursor polymer: oxidative coupling with FeCl ₃	29
2.4 Preparation of precursor polymer with Suzuki cross-coupling	29
2.3 Preparation of post-functionalized polymers	30
3. CHARACTERIZATION	31
3.1 Physical properties	31
3.2 NMR characterization	32
3.3 UV-Vis spectroscopy.....	34
3.4 Electrochemical properties.....	36
3.5 Organic solar cells	38
CONCLUSION	40
EXPERIMENTAL PART	42
1. MATERIALS AND METHODS	44
Synthesis of monomers: transesterification reaction	46
3-(6-Bromohexyloxy)thiophene (1a).....	46
3,4-(6,6'-Dibromohexyloxy)thiophene (2a).....	47
Synthesis of monomers: dibromination reaction	48
2,5-Dibromo-3-(6-bromohexyloxy)thiophene (1b).....	48
2,5-Dibromo-3,4-(6,6'-dibromohexyloxy)thiophene (2b).....	49
Synthesis of precursor polymers: oxydative coupling with FeCl ₃	50

<i>Poly{3-(6-bromohexyloxy)thiophene-co-3-[5-(4-phenoxy)-10,15,20-triphenylporphyrinyl]hexylthiophene} (P1a-TPP)</i>	50
<i>{3,4-(6,6'-dibromohexyloxy)thiophene-co-3-[5-(4-phenoxy)-10,15,20-triphenylporphyrinyl]hexylthiophene} (P2a-TPP)</i>	51
<i>Synthesis of precursor polymer: Suzuki cross-coupling reaction</i>	53
<i>Poly4-[3,4-(6,6'-dibromohexyloxy)thiophen-2-yl]benzo[c][1,2,5]thiadiazole (P2b-Bz)</i>	54
<i>Synthesis of ionic polymers: post-functionalization reaction with PBU₃</i>	55
<i>Poly{3-(6-tributylphosphoniumhexyloxy)thiophene-co-3-[5-(4-phenoxy)-10,15,20-triphenylporphyrinyl]hexylthiophene bromide} (P1a-buP)</i>	55
<i>Poly{3,4-(6,6'-tributylphosphoniumdihexyloxy)thiophene-co-3-[5-(4-phenoxy)-10,15,20-triphenylporphyrinyl]hexylthiophene bromide} (P2a-buP)</i>	56
<i>Poly4-[3-(6-tributylphosphoniumhexyloxy)thiophen-2-yl]benzo[c][1,2,5]thiadiazole (P1b-buP)</i>	57
<i>Poly4-[3,4-(6,6'-tributylphosphoniumdihexyloxy)thiophen-2-yl]benzo[c][1,2,5]thiadiazole (P2b-buP)</i>	58
4. ORGANIC SOLAR CELLS	59
REFERENCES	61

Introduction

1. Foreword

As the energy demand continues to rise, especially from developing countries, there is a constant and global urgency to reduce emissions of CO₂ and other harmful substances, as well as to fight the greenhouse effect. While coal appears to last about 150 years at current production levels, proven oil and gas reserves could only be available for about one-third of this period. However, opinions differ as to whether oil production will peak. For the International Energy Agency (IEA), which advises Western economies on energy policy, the peak production should not be reached before 2040. Whereas low-grade coal and bituminous residues are expected to last from one to two centuries, but with greater problems of energy efficiency and atmospheric pollution. Fortunately, by 2030, nearly one-third of Europe's energy will have to come from renewable sources. Moreover, not only will the climate benefit from this green growth, but the countries which have been the most ambitious in improving wind and solar energy are also experiencing a sharp decline in terms of electricity prices. Presently, the most popular alternative source of energy for households is the solar energy converted into electricity by photovoltaic panels. However, due to the rising quest of it, innovations based on new technologies - that are more efficient and economical than current silicon-based technologies - are therefore necessary, to become the main source of global energy generation. To address this problem, several efforts have been recently made to produce efficient and cost-effective photovoltaic devices using organic materials. Indeed, thanks to the use of polymers as semiconductor materials, chemically manipulable solar cells can be produced with lower processing and raw material costs.¹⁻⁵

2. Conjugated polymers

2.1 Overview

Conductive polymers are a new class of materials which exhibit highly reversible redox behavior and combine the typical properties of plastics (i.e., lightness, corrosion resistance, workability, etc.) with those of metals (i.e., electric properties), that ordinary polymers usually do not have. The usefulness of conducting polymers and their successful application in an increasing number of technologies, such as biomolecular electronics, telecommunications, as well as display devices and electrochemical storage systems, has further increased the interest of researchers in this new field. Conductive polymers can be classified into two categories:

- extrinsically conductive polymers (ECPs);
- intrinsically conductive polymers (ICPs).

ECPs are ordinary polymers but doped with powders of electrically conductive metals, such as copper and gold or graphite. In these polymers, the percentage of doping mass can be up to 50% of the total mass, which is much more than inorganic semiconductors, where the maximum doping commonly reaches 5%. On the other hand, ICPs are conjugated polymers and therefore present, in their main chain, the alternation of single and double bonds, which leads to electronic delocalization fundamental to conductivity.

The first ICP studied was polyacetylene (PA), whose conductive properties were discovered in 1977 by Heeger, Mc Diarmid and Shirakawa, who made PA electrically conductive by suitable doping. The main ICPs are polyparaphenylene (PPP), polyparaphenylenevinylene (PPV), polyaniline (PANI), polyparaphenylene sulfide (PPS), poly-3-alkylthiophene (P3AT), polypyrrole (PPy), polyisothianaphthene (PITN), and polyethylenedioxythiophene (PEDOT) (Figure 1).^{6,7}

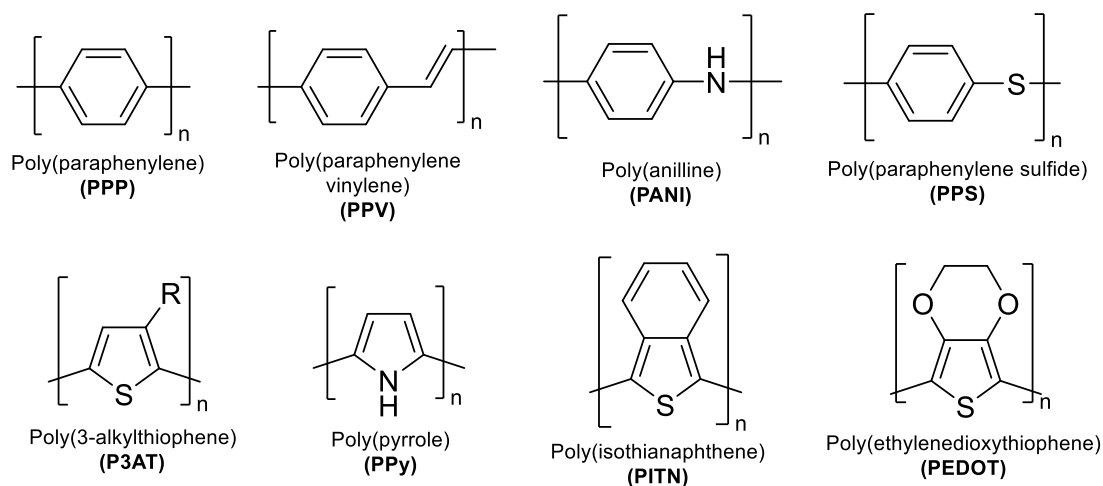


Figure 1. Structures of the main conjugated polymers used in organic electronics.

2.2 Conductivity and charge transport

The electrical and conductive properties of conjugated polymers can be explained by the "band model" used for inorganic semiconductors. The conjugated structure consists of an alternation of single (σ) and double (π) bonds that can be shifted along the structure by the resonance effect. Since the carbon atoms are hybridized (sp^2), there are p_z orbitals which are parallel but perpendicular to the plane of the sigma bond: each of these orbitals contains an unpaired electron that can overlap laterally, creating a bonding (π) and an antibonding (π^*) orbital. When the number of conjugated double bonds increases, nearly isoenergetic levels are formed thus creating two bands, the valence band (VB) and the conduction band (CB), whose energy difference is defined as the energy gap (E_g).

The conductive properties of materials are therefore classified according to the energy gap. If the energy gap between the valence band and the conduction band is quite reduced, the material can be considered a semiconductor; instead, when the two bands are overlapped or very close in terms of energy, the material is a conductor. Finally, if the energy gap is too large, the material results to be an insulator, since it is impossible to transport an electron from the valence band to the conduction band, even when external stimuli are present. The π -conjugated polymers are considered semiconductors because their energy gap is of the order of 1 eV. To occur electrical conduction, i.e., the transfer of electrons from the valence band to the conduction band, an external excitation must be present, i.e., in the form of photoexcitation, thermal excitation, or the action of dopants.^{8,9}

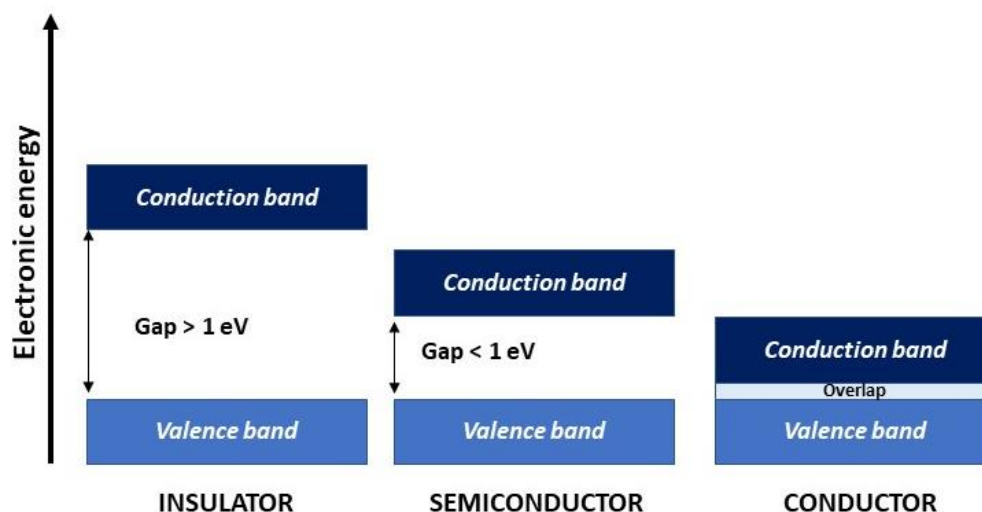


Figure 2. Schematic representation of E_g for insulating, semiconductor and conductive materials.

2.3 Doping

To achieve good conductivity, the distance between VB and CB must be reduced so that electrons can be excited into the conduction band. This can be possible by the reversible process of doping of the neutral polymer through its oxidation or reduction.

In the case of inorganic semiconductors, no charge transfer takes place, and doping means that the dopant is introduced into the semiconductor lattice, creating electron-rich and electron-poor sites. By contrast, doping in conjugated polymers is reversible because they have high electron affinity and low ionization potential, allowing the acquisition and removal of electrons with acceptable amounts of energy.

The charge in inorganic semiconductors is carried by electrons, while in conductive polymers the species responsible for conductivity are polarons and bipolarons, cationic or anionic, depending on the type of doping.

When the oxidative doping (p-doping) takes place, the molecule acquires a positive charge as the electron accepting species remove an electron π , forming a vacancy and a radical cation. Commonly used electron acceptor are Lewis acids (AlCl_3 , FeCl_3 , etc.), strong protonic acids (or salts), and halogens. As being very unstable, the formed radical cation is delocalized along a polymer fragment by resonance, to separate the positive charge from the unpaired electron and form an extended quinoid structure, with 4 or 5 thiophene rings (polaron). In the case of strong doping, two radical cations can interact with each other and form a dication (bipolaron) (Figure 3).

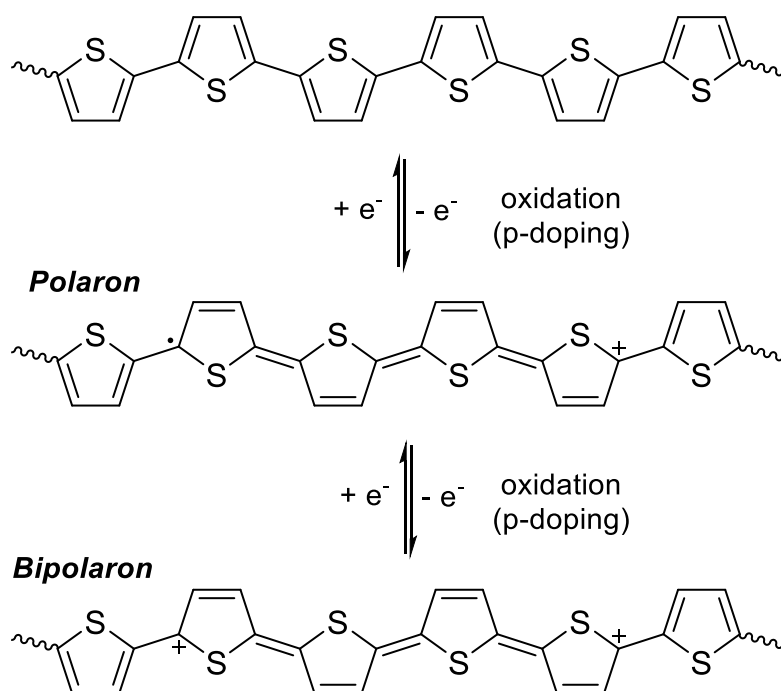


Figure 3. Formation of polaron and bipolaron in polythiophene.

On the other hand, with a n-doping (reductive doping) the reducing species leads to the formation of a complex in which the polymer is negatively charged and balanced by a positive counterion. The electron donor species donates a π -electron to the polymer, creating a radical anion that evolves into an anionic polaron and, in the case of heavy doping, a dianion. The main electron donor species are alkali metals in the gas phase (Na, K, etc.) or liquid ammonia. The presence of polaron and bipolaron produce delocalized structural deformations (quinoid forms), with a destabilization of the bond orbital, and therefore creation of real bipolaron bands at an intermediate energy between the valence and conduction bands, which determines conductivity in conjugated polymers.

The factors that most affect the conductivity of ICPs are:

- the percentage of doping agent;
- the orientation of the polymer chains: due to the presence of anisotropy, a chain conducts better current in one direction than the other. Besides, conductivity is highest when the chains are aligned parallel to each other, thus allowing a general intra-chain charge transport, but mechanisms involving electron jumps from one chain to another are also possible (hopping);
- the presence of structural defects (i.e., sp^3 hybridized carbon atoms), limited planarity and/or chain regio-irregularities (i.e., head-to-head (HH) or tail-to-tail (TT) connections);
- the presence of impurities that prevent the passage of electrons through the polymer chain.^{10,11}

3.2 Optical properties

Depending on the conformation of the polymer chains and their interactions, π -conjugated materials are characterised by different optical properties that can be easily tuned by chemical modifications. For example, the presence of oxygen directly connected to the thiophene ring injects more charge into the system and stabilises the macromolecular chain, leading to a further decrease in the HOMO-LUMO band gap of the material and absorption of radiation at lower energy (Figure 5A). Similarly, the alternation of electron donor (ED) and electron attractor (EA) units in the conjugated system with main chain usually leads to a strong decrease in the band gap, as internal orbital mixing seems to take place (Figure 5B). On the other hand, the insertion of certain substituents in the side chain, such as porphyrin derivatives, which exhibit very strong absorption in the blue-violet region of the spectrum, offers the possibility of increasing and broadening the absorption spectrum of the material (Figure 5C).^{17,18}

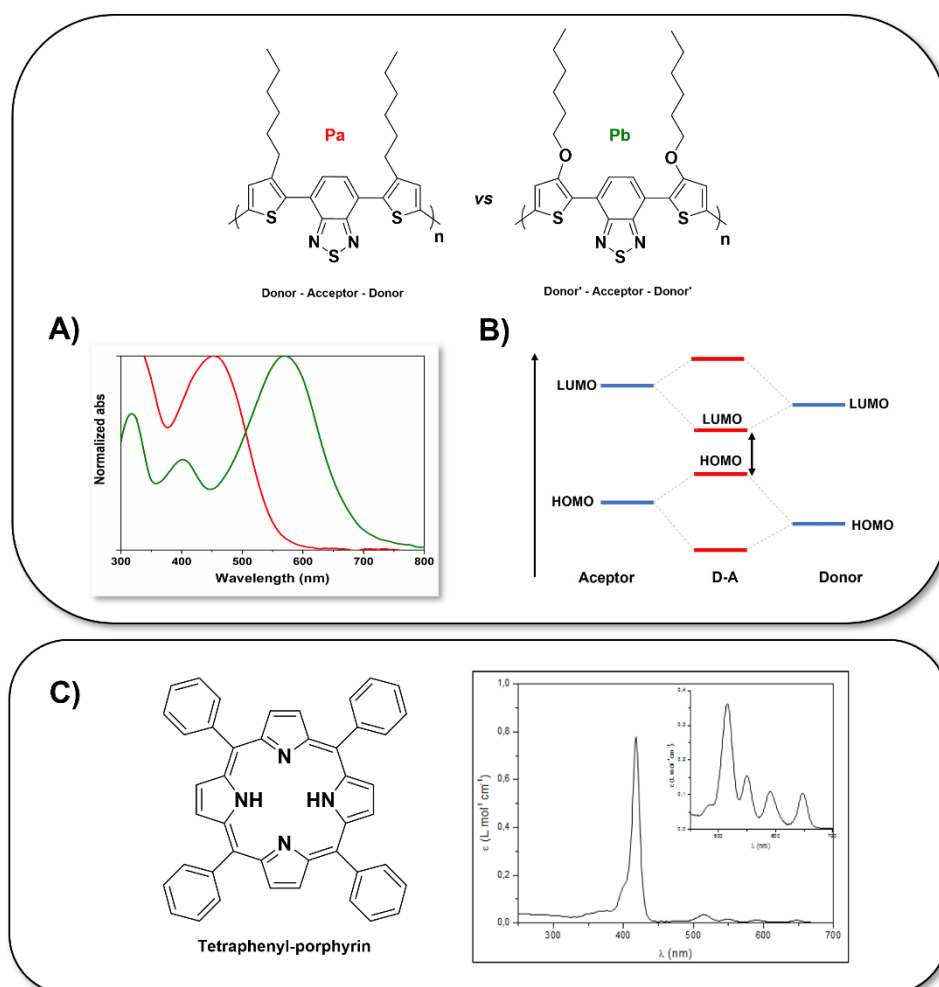


Figure 5. A) Effect on the optical properties of the insertion of oxygen atom into a π -conjugated material; B) representation of the internal orbital mixing in alternated ED-EA π -conjugated material; C) typical UV-Vis profile of a porphyrin derivative.

The optical properties of the material can also be modified by external stimuli, due to different phenomena of chromism (i.e. electrochromism, thermochromism and solvatochromism).

Electrochromism consists in the colour change of the polymer depending on its oxidation state. The π -conjugated polymers, when subjected to electrochemical oxidation or reduction, undergo a p- or n-doping process. As mentioned before, new energy states are created between the valence and conduction bands, leading to a decrease in the energy associated with the electronic $\pi \rightarrow \pi^*$ -transition. In addition, the doping of the polymer leads to a transition from aromatic to quinoid form, which favours the adoption of a planar conformation. Since planarization leads to absorption at lower energy and thus at a longer wavelength, the doped polymer shows a different colour than in the neutral state. Polythiophenes usually show a red-orange colour in their neutral form and a blue-green colour when doped.

The phenomenon of *thermochromism* occurs when the colour of the polymer changes in the solid state due to a change in temperature. Namely, an increase in temperature results in a transition from an ordered, planar main chain conformation to a partially rotated, and thus distorted, conformation with a shorter average conjugation length, due to an increase in disorder in the side chains.

Solvatochromism, on the other hand, is a phenomenon observed when a non-solvent is slowly added to a polymer solution. As a consequence, the polymer chains are desolvated and thus organized in more ordered and planar conformations, with lower internal energy.

Indeed, since the energy difference between the π - π^* orbitals - responsible of the electronic transitions in the visible spectrum - is inversely proportional to the extent of conjugation of the polymer chains, any structural changes result in a colour change of the polymer. Specifically, a red shift (or bathochromic shift) occurs when the electronic transition absorbs at longer wavelengths and the polymer exhibits a blue-green colour; while a blue shift (or ipsochromic shift) occurs when the absorption shifts to shorter wavelengths and the polymer exhibits a red-orange colour.

The great feature of these phenomena is their reversibility, as the polymers display their original optical properties when the external stimuli are removed.^{8,19}

3.3 Synthesis of P3ATs

Starting from mono- or oligo-thiophene based monomers, generally functionalized with alkyl side chains in the β -position to ensure solubility of the final polymer, the synthesis of P3ATs is possible by electrochemical or chemical methods. Besides, to obtain a polymer with electron delocalization along the main chain, the thiophene rings must be linked together in the α -position: it is therefore possible to divide the main synthetic routes into not-specific and regiospecific methods.

3.3.1 Oxidative polymerization with $FeCl_3$

With this not-regiospecific oxidative synthesis, the thiophene monomers react with $FeCl_3$, that both acts as a polymerizing agent and an oxidizing agent (i.e., a dopant).

Firstly, a solvent in which the oxidant is insoluble (CCl_4 or $CHCl_3$) need to be used, to guarantee the Lewis acid character of iron atom (empty d orbital), thus allowing the coordination of the thiophene monomer via the free electron pairs on the sulphur atom. Then the oxidizing agent is generally used in large excess (four times the number of moles of the monomer), since it is both used for the formation of the oxidized polymer and for the reaction with the resulting HCl.

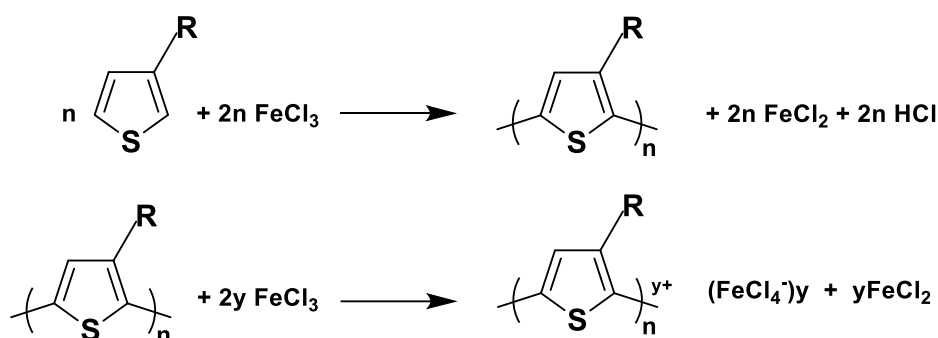


Figure 6. Scheme of the oxidative polymerization with $FeCl_3$.

Besides, to prevent oxygen from interfering with the reaction mechanism, as well as to remove the formed HCl that could degrade the product, the reaction is conducted under inert atmosphere. This synthesis guarantees good yields, high molecular weights and typically allows to obtain a polymer with a percentage of regioregularity between 70 and 80%. However, due to the poor control of the final molecular weight, the reproducibility of this method is one of its major issues.^{14,20}

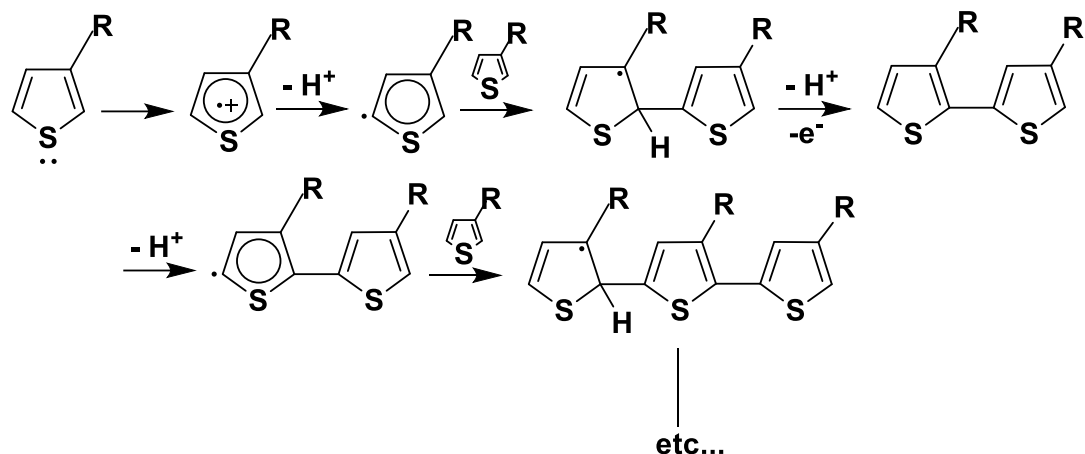


Figure 7. Mechanism of the oxidative polymerization with $FeCl_3$.

3.3.2 Suzuki cross-coupling polymerization

Regioregular polythiophenes can be synthesized by means of transition metal-catalysed polymerization, for example exploiting the Suzuki reaction. This method involves a cross-coupling reaction with Pd as a catalyst, and boron reagents as organometallic intermediates (Figure 8).

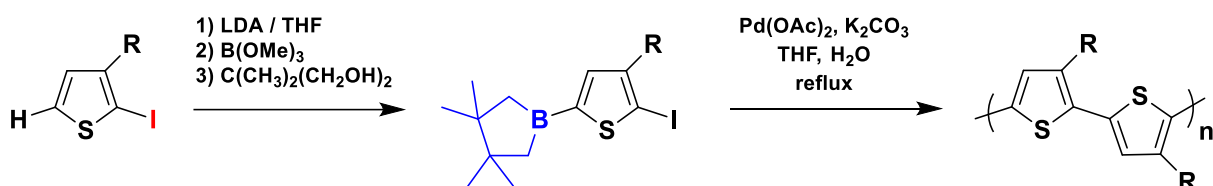


Figure 8. Polymerization scheme via Suzuki cross-coupling.

The most commonly used Pd complex (i.e., $Pd(PPh_3)_4$) is generally very reactive due to the bulky and electron-donating ligands (e.g., PPh_3), in addition to the free coordination site of the complex, which leads to an intermolecular mechanism of oxidative addition (OA). Indeed, the first step of the cycle is an OA in which the active species (Pd^0) attaches to the aryl carbon atom of the halide; the insertion of palladium weakens the C-X bond as the palladium oxidises and changes from $Pd(0)$ to $Pd(II)$, donating two electrons to an antibond orbital of the electrophilic species. Then the second phase corresponds to a trans-metalation (TM) step in which the boron-containing organometallic derivative coordinates to the metal centre, thus exchanging their ligands (halogen and organic group). Since the boron species has a weak carbanionic character, $NaHCO_3$ or $NaOH$ as base is then added to coordinates with the boron and weakens the bond with the carbon. In the third and final step, reductive elimination (RE) occurs with electronic rearrangement of the complex, formation of the C-C bond between the two aromatics, and regeneration of the catalyst (Figure 9).

With this method HT coupling rates exceeding 96-97% are commonly achieved, but cryogenic conditions are usually required for the preparation of the intermediates, which must also be isolated and purified.^{20,21}

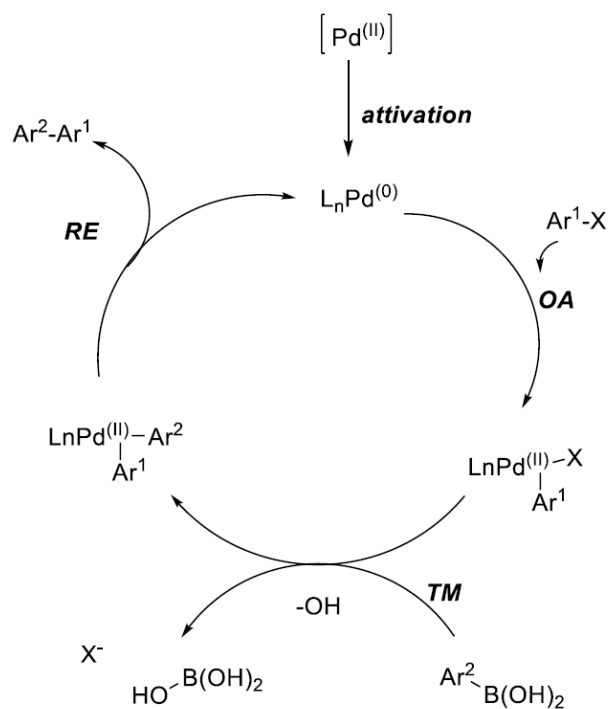


Figure 9. Pd catalysed mechanism for a Suzuki polymerization.

4. Application of ICPs

As organic semiconductors, π -conjugated polymers are mainly used as electroactive materials for nonlinear optics and electronics. In particular, among all the possible various applications of these polymers (i.e., batteries, electrochromic devices ECDs, organic light-emitting diodes OLEDs, etc.), the one of organic photovoltaic cells (OPVs) is here discussed in this dissertation.

4.1 Organic Photovoltaic Cells (OPV)

4.1.1 Solar energy

The sun radiates onto the earth's surface a large amount of energy (120000 terawatts), which is 6000 times the current global energy consumption (20 terawatts). Solar energy is abundant, but has low intensity and it is intermittent, as being affected by weather conditions and the alternation of day and night. Moreover, since it passes through the atmosphere, the solar radiation result to be attenuated, because part of it is reflected and absorbed (mainly by water vapour and other atmospheric gases), while the remaining portion is partially scattered by the air and solid particles suspended in the air. Thus, the radiation reaching the Earth's surface is finally composed of:

- direct radiation;
- diffuse radiation, which reach the surface from the sky in all directions;
- reflected radiation, from the ground and the surroundings of a given surface.

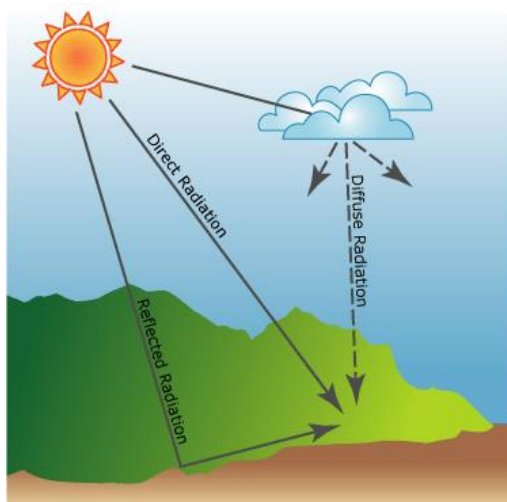


Figure 10. Illustration of the solar radiation incident on the Earth's atmosphere.

4.1.2 Mechanism of photogeneration

The working mechanism of photovoltaic cells is based on the photovoltaic effect, which states that a photon absorbed by the material causes an electron promotion from the valence band to the conduction band, leaving a hole in the less energetic band. This creates an electron-hole pair, which must diffuse through the material and reach the two electrodes to generate current. The electrons move through the device toward a positively charged electrode (anode), while the holes move toward the opposite electrode (cathode). For a transition to occur between the bands, the electron must receive a minimum amount of energy equal to the energy band gap of the material.

The previously described mechanism of photogeneration is valid for inorganic silicon-based devices, but it is slightly different for solar cells made of organic material. In the latter case, the interaction between the generated charges of opposite sign - resulting from light absorption - is stronger, due to the lower dielectric constant of the material. This hole-electron pair is called *exciton* and interacts via the Coloumb force. Excitons can spontaneously meet and recombine, or relaxing via a photoemitting mechanism and radiatively decay to the ground state by spontaneous emission, thus dissipating the energy provided by the photon.

An efficient dissociation of excitons is therefore necessary and requires strong electric fields, which can be generated by a two-component system consisting of an electron donor and an electron acceptor material. Typically, the ED material has a high ionization potential (IP), which is the energy required to remove an electron from the HOMO orbital of a neutral material; by contrast, the EA material must have a high electron affinity (Eaf), which is a measure of its ability to act as an electron attracting material.^{15,22–25}

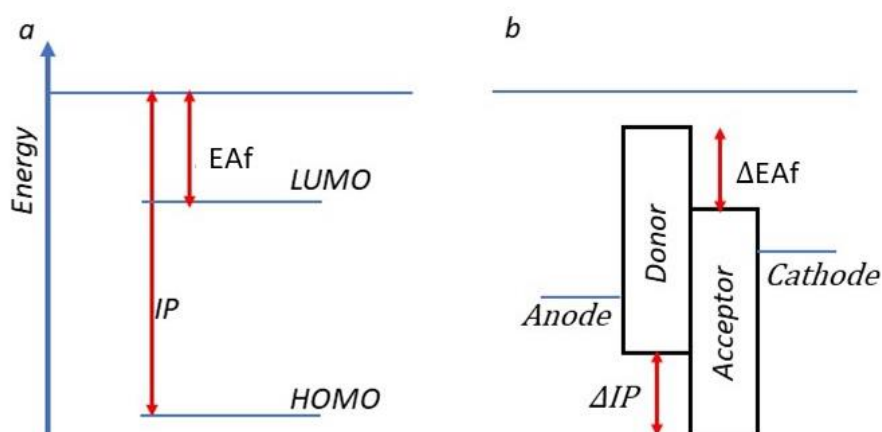


Figure 11. Energy diagram for an organic semiconductor (a) and a blend of donor-acceptor materials (b).

The operating mechanism for an OPV thus consists of four steps (Figure 12):

1) Photoabsorption

A photon beam hits the donor material and promotes an electron from its HOMO orbital (valence band) to the LUMO orbital (conduction band), creating an exciton. To optimise this step, the ED semiconductor material should have a reduced energy gap between VB and CB, so that it can absorb a larger fraction of solar radiation.

2) Diffusion

Due to a chemical potential, the exciton must then diffuse in the donor material at the interface with the acceptor material before decaying to the ground state and losing the absorbed energy.

3) Hopping

Electron transfer from the LUMO orbital of the donor to the LUMO orbital of the acceptor have to occur, forming a charge transfer complex. To be possible, the acceptor's VB and CB must fall sequentially on both the donor's VB and VB. Besides, the energy offset between the two LUMOs (ΔEA) must be less than the binding energy of the exciton (otherwise the charges could recombine, reducing the efficiency of the mechanism).

4) Transport of the charge carriers to the electrodes

At the ends of the cell, the charge transport complexes break apart and free charges are formed, as the distance between the electrons and the electron holes becomes larger than the Coulomb attraction radius. After charge separation, the holes and electrons are attracted and collected to the electrodes of opposite sign, where they can complete the process of converting radiant energy into electrical energy in an external circuit.^{26,27}

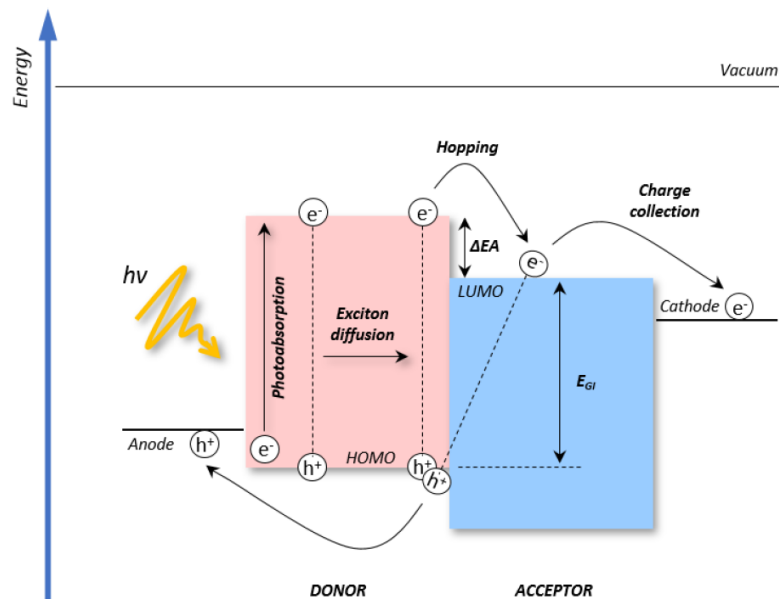


Figure 12. Scheme of the device operating principles.

4.1.3 Acceptor-donor materials

In organic photovoltaic cells, the active layer is typically made of a blend of electron-donor and -acceptor materials. While the ED component is commonly a conjugated polymer or small molecule, the most used EA material is a fullerene derivative, such as PC₆₁BM (phenyl-C₆₁-butyric acid methyl ester) or its derivatives. An example of a donor material used in OPVs is poly(3-hexylthiophene) (P3HT), a conjugated polymer that has been widely used in OPVs due to its high charge carrier mobility and good compatibility with fullerene acceptors. However, despite P3HT has an excess of electrons due to the presence of thiophene rings, which can donate electrons to the acceptor material, the performance of OPVs made with this polymer depends on its regioregularity and process conditions.

To improve the device performances, alternative ED polymers to P3HT - with smaller band gaps and higher charge mobility - have been thus developed and investigated for the use in OPV cells. Some examples of this alternatives include: Poly(2,5-bis(3-alkylthiophen-2-yl)thieno[3,2-b]thiophene) (PBTTT), Poly(2,7-carbazole) (PCz) (Figure 13), Poly(3-butylthiophene) (P3BT) and Poly(3-hexylselenophene) (P3HS) that have higher absorption coefficient and higher charge carrier mobility than P3HT.

Instead, the commonly used acceptor material in OPVs are fullerene derivatives or non-fullerene organic molecules. Fullerene materials such as PC₆₁BM (phenyl-C₆₁-butyric acid methyl ester) and PC₇₁BM (phenyl-C₇₁-butyric acid methyl ester) have been widely used, due to their high electron

mobility and good compatibility with many donor materials. In particular, PC₇₁BM has a higher molecular weight and a larger molecular size than PC₆₁BM, which can result in better absorption of light and improved charge transport properties. However, PC₇₁BM is more expensive and less soluble in organic solvents compared to PC₆₁BM.

For this reason, non-fullerene acceptor (NFAs) materials have recently emerged as promising alternatives to fullerene derivatives, due to their tuneable energy levels, strong absorption in the visible and near-infrared regions, and potential for high efficiency. Examples of NFAs used in OPVs include: ITIC (Indacenodithieno[3,2-b]thiophene) (Figure 13), IDIC (Indacenodithieno[3,2-b]thiophene-2,8-dicarboximide), Perylene diimide (PDI). All these molecules have strong absorption in the visible region and high electron mobility, which enables efficient charge transport and collection.

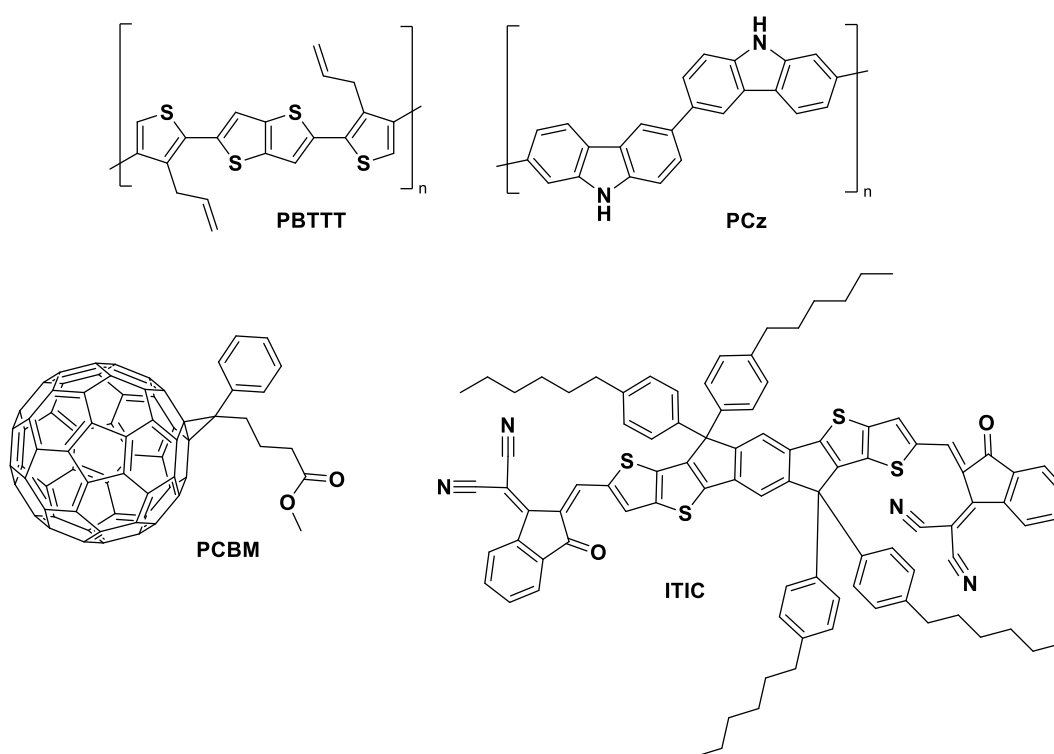


Figure 13. Alternative donor materials in BHJ organic solar cells

The choice of acceptor material in OPVs depends on several factors such as the desired energy level alignment with the donor material, the absorption spectrum, and the charge transport properties.^{25,28}

4.1.4 BHJ architecture

There are different types of solar cells, but all of them are made by layer deposition and thus sandwich construction, where the active layer is always placed between two electrodes.

The first devices developed were the *single-layer* and the *double-layer* solar cells; in the first case there is a single layer of conducting polymer, while in the second case two layers of donor and acceptor polymer/material are brought into contact with each other, forming an interface. Both structures are limited by the scattering length of the exciton, which must not exceed 20 nm, otherwise recombination would occur. Moreover, this limits the thickness of the active layer as well as the fraction of the incident light that can be absorbed. To increase efficiency, a third type, the so-called *bulk heterojunction* (BHJ), had to be developed (Figure X).

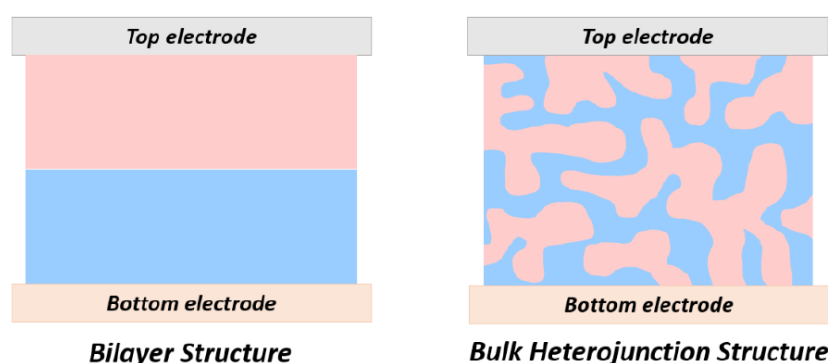


Figure 14. Fundamental architectures of photoactive layer.

BHJ cells are a type of OPVs widely used for converting light into electricity. Composed of a blend of a donor and an acceptor material, the two components are mixed in a random fashion to form a nanoscale network of interpenetrating domains. In addition to be easy-processable and flexible, this architecture creates a large interfacial area between the ED and EA, improving the charge separation and collection.^{29,30}

Among OPVs with BHJ architecture, different geometries/configurations are possible:

- *Standard BHJ*, when the donor and acceptor materials are mixed together without specific arrangement or patterning. This creates a disordered, interconnected network of nanoscale domains throughout the active layer with a large interface between the two components. The standard, and thus random, BHJ geometry is the most commonly used because it is easy to fabricate and can achieve high energy conversion efficiencies. However, the random nature of the mixture can also lead to morphological disorder, which can cause inefficiencies in charge transport and recombination. To mitigate these effects, different strategies were adopted, such as

optimizing the ratio of ED/EA, using solvent additives, or incorporating additives or functional groups to improve compatibility between the two components.

- *Tiered Graded BHJ*, when the composition of ED/EA is gradually varied across the active layer, creating a gradient of energy levels and morphology. In addition to improve charge separation and transport, the graded structure can also reduce the impact of morphological disorder on device performance. This configuration may be created i.e., by changing the ratio of D/A, by using a solvent gradient, or by depositing the blend with a controlled pattern. The gradient can be linear or nonlinear. Despite graded BHJs have shown promise in improving the charge transport and reducing recombination losses, their fabrication can be more complex and challenging than that of random BHJs, since it requires precise control of the composition and morphology of the mixture. In addition, optimization of gradient structures often requires extensive experimentation and modeling to determine the optimal gradient profile for a given set of materials and device parameters.
- *Tandem BHJ*, when two or more BHJ layers with complementary absorption profiles are combined and stacked to create an OPV with multiple junctions. In a tandem BHJ, the top layer typically has a higher bandgap energy and absorbs light of shorter wavelengths, while the bottom layer has a lower bandgap energy and absorbs light of longer wavelengths. The two layers are connected by a cascade of intermediate layers that facilitate charge transfer between the various junctions. Each layer could have its own ED and EA materials, or they may share one of the materials for a better compatibility. The design and optimization of tandem BHJ devices can be complex and challenging, as the bandgap energies, absorption spectra, and morphology of each layer, as well as the electrical and optical properties of the interlayers, must be carefully considered. Nevertheless, tandem BHJ structures have shown significant potential for improving the efficiency and stability of OPVs, achieving efficiencies above 17% in lab-scale devices.
- *Inverted BHJ*, when the layer order is reversed. This configuration may have some advantages over the conventional BHJ, including higher stability, better charge transport, and easier fabrication. Inverted BHJs also often use a different electrode architecture, such as a transparent conductive oxide (TCO) layer over the active layer, which enables better charge collection and lower recombination losses. Moreover, the inverted structure can allow the use of thicker donor layers, which can improve light absorption and increase the overall efficiency of the device.^{26,31}

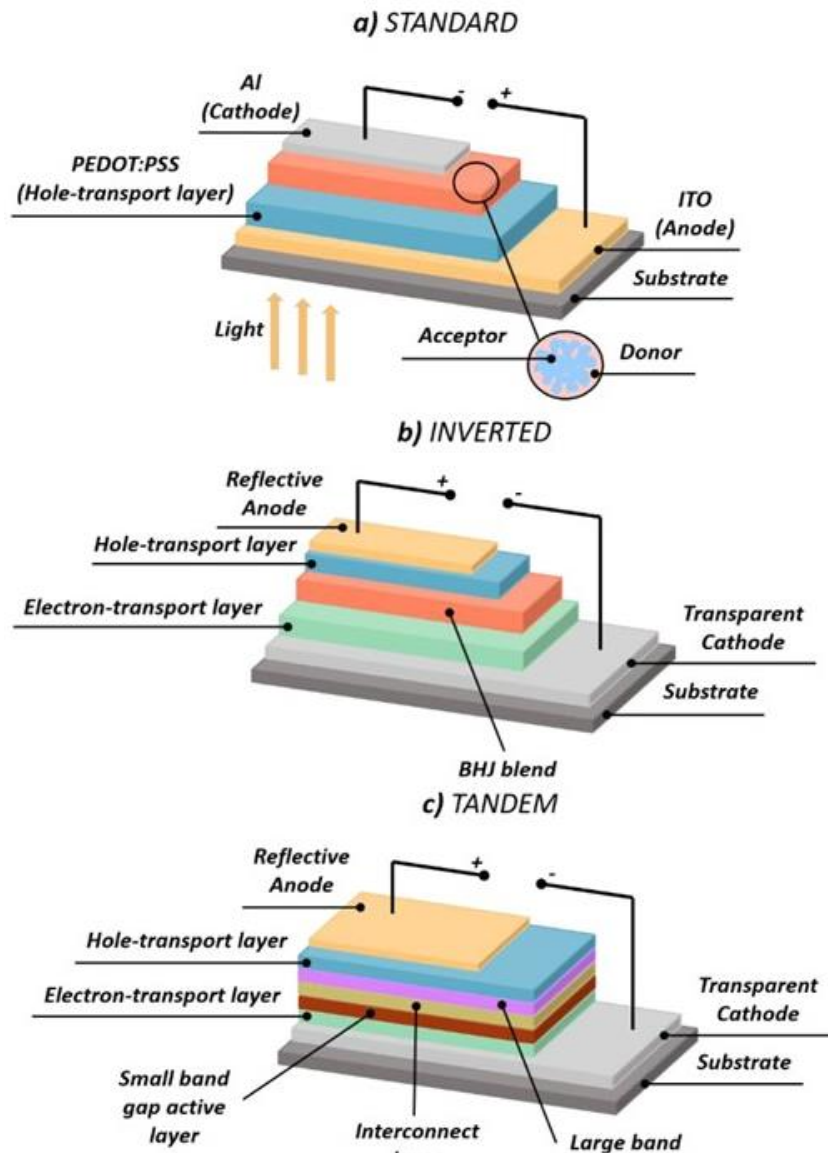


Figure 15. Device geometry of (a) standard, (b) inverted and (c) tandem OPV cells.

5. Interlayer material

An interlayer material, also known as an interfacial layer, is a thin layer of material commonly placed between the photoactive layer and the electrodes, to further improve the performance of the device. In addition to work in OPVs, interlayers can also be used in a variety of electronic devices, including organic light-emitting diodes and transistors (OFETs).

The functions of an interlayer material depend on the specific application and the properties of the adjacent layers. In some cases, an interlayer could act as a barrier layer, preventing the diffusion of impurities, or as a charge carrier between adjacent layers. In other cases, an interlayer could act as a buffer layer, smoothing the interface between two dissimilar materials, with different lattice structures or thermal expansion coefficients.

Generally, in organic electronic devices, interlayer materials are often used to improve charge transport and collection, in order to reduce the energy barriers at the interfaces between the different layers. For example, in OPVs, an interlayer should improve the contact between the ED and EA materials, facilitating charge separation and collection. Whereas in OLEDs, an interlayer material may be used to improve the injection of charge carriers from the electrodes into the organic layers, enhancing the efficiency and brightness of the device.

Common interlayer materials used in organic electronic devices include metal oxides (such as titanium oxide and zinc oxide), polar conjugated polymers (i.e., poly(3,4-ethylenedioxythiophene) polystyrene sulfonate, PEDOT:PSS) and small organic molecules. The choice of the material depends on factors such as the properties of the adjacent layers, the device architecture, and the desired performance characteristics^{31,32}.

Results and Discussion

1. Aim of the work

As previously mentioned, due to the progressive and continuous depletion of fossil fuels, the attention is presently focused on renewable energy sources, including solar power. In particular, since the cost of the currently commercially available inorganic photovoltaic cells is quite high, the development of alternative materials such as π -conjugated conductive polymers is definitely increasing. However, despite this class of materials present many advantages as discussed in the introduction part, their production often requires the use of not “environmentally friendly” conditions, because of their solubility in toxic solvents. In this context, materials that combine excellent optical properties with green solubility are thus object of investigation and study.

Therefore the aim of the master’s internship, carried out in the Polymers Research Group of the "Toso Montanari" Industrial Chemistry Department, was about the synthesis, study and application of ionic heteroalkyl alcohol-water soluble thiophene based materials, for application as cathode interlayer in halogen-free OSCs of BHJ type (Figure 1).

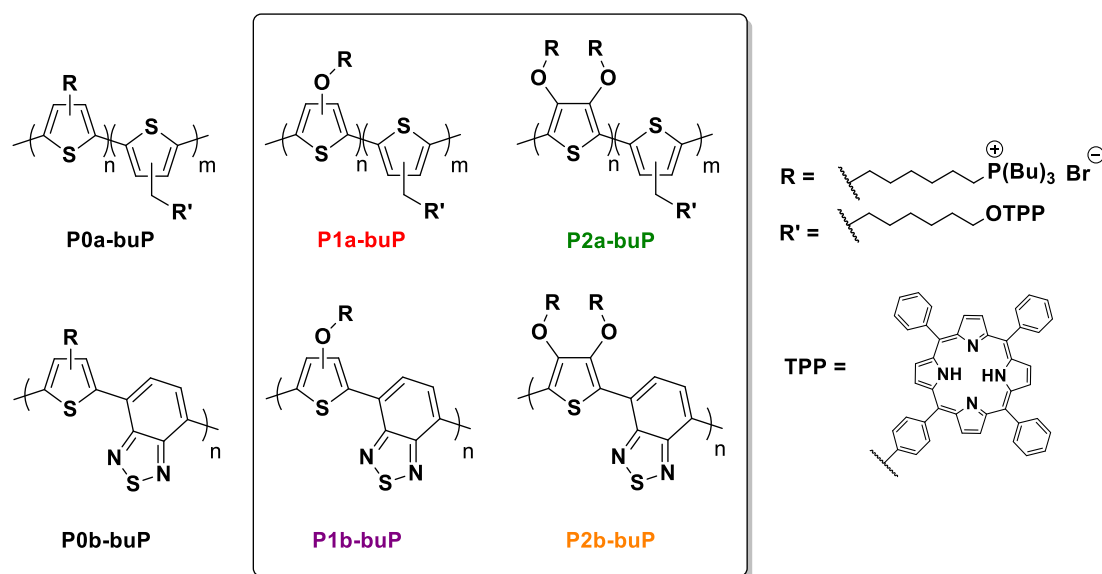


Figure 1. Overview of the prepared ionic heteroalkyl alcohol-water soluble thiophene based materials (**P1a-buP**, **P2a-buP**, **P1b-buP** and **P2b-buP**): the study was performed by comparison with two materials having similar structure but no oxygen in the side chain (**P0a-buP**, **P0b-buP**).

In particular, the evaluation, comparison and fine-tuning of the energy level alignment was obtained by:

- insertion of one or two oxygen atoms directly linked to the thiophene ring, with the aim to shift the absorption towards the infrared;
- the design of main-chain alternated ED-EA (push-pull) single materials, thus polymers with small band-gap;

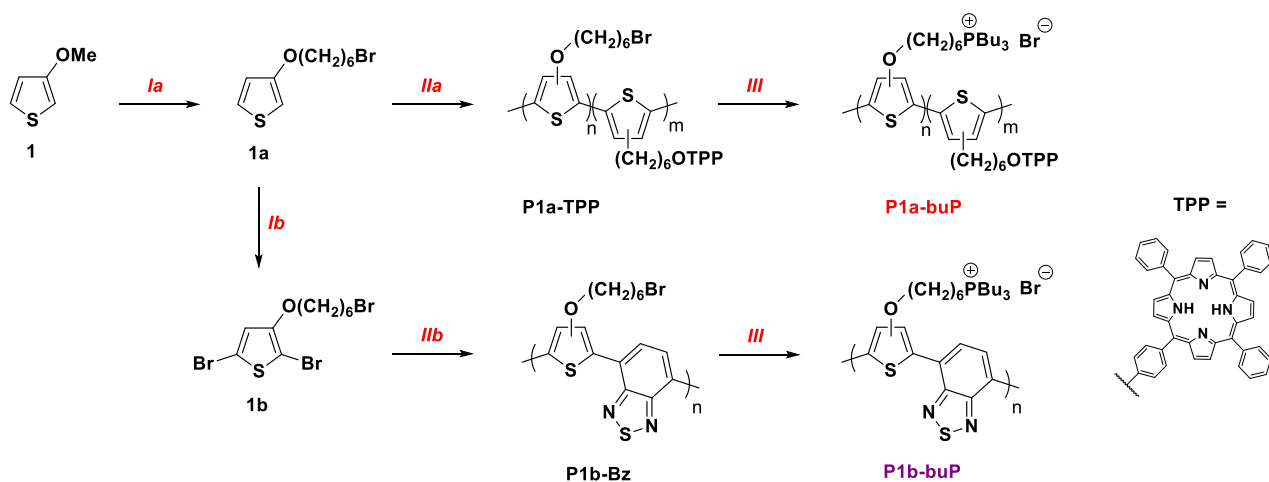
- insertion of a dye sensitizer (i.e., tetraphenyl-porphyrin, TPP) into the side chain, to extend the absorption profile, as well as positively influencing the morphology of the material.

Besides, the solubility in green solvents of all synthesized materials was guaranteed by post-functionalization approach, with the insertion of ionic alcohol/water-soluble phosphonium salts in the side chain.

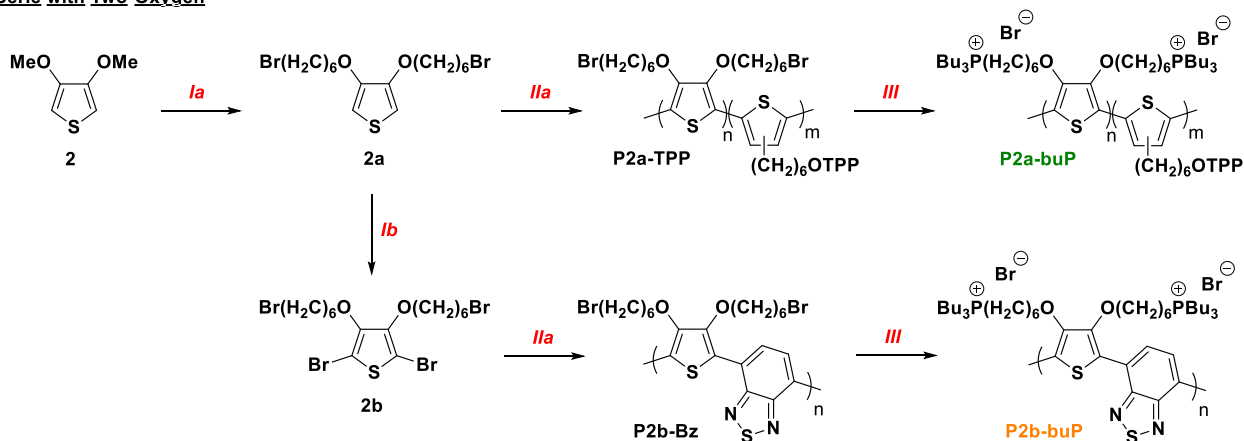
2. Synthesis

Starting from oxyalkyl-thiophene derivatives (**1a** and **2a**), two different class of precursor copolymers were obtained. Specifically, in presence of 3-[5-(4-phenoxy)-10,15,20-triphenylporphyrinyl]hexylthiophene (**T6OTPP**, previously prepared by the research group), dye-sensitized copolymers were synthesized by oxidative coupling with iron trichloride (**P1a-TPP** and **P2a-TPP**). Whereas, by previous dibromination of monomers to afford **1b** and **2b**, alternated ED-EA main-chain copolymers were prepared in presence of 2,1,3-benzothiadiazole-4,7-bis(boronic acid pinacol ester) (**Bz**, commercially available), by Suzuki cross-coupling reaction (**P1b-Bz** and **P2b-Bz**). Finally, ionic alcohol-soluble polymers were synthesized by a post-functionalization approach with tributyl phosphine (Scheme 1).

Serie with One Oxygen



Serie with Two Oxygen



Scheme 1. Synthetic routes to obtain monomers and copolymers by transesterification (*Ia*), dibromination (*Ib*), oxidative coupling with FeCl₃ (*IIa*), Suzuki cross-coupling reaction (*IIb*) and post-functionalization with PBU₃ (*III*) reactions.

2.1 Preparation of the monomers

The heteroalkyl-thiophene based monomers (**1a** and **2a**) were synthesized by trans-etherification of the commercially available 3-methoxythiophene (**1**) or 3,4-dimethoxythiophene (**2**), in the presence of 6-bromo-1-hexanol (**B6OH**, previously prepared by the research group) and a catalytic amount of p-toluenesulfonic acid. Then, in order to perform a Suzuki cross-coupling polymerization, a part of the obtained monomers was subsequently dibrominated with N-bromosuccinimide, an easy handling solid reagent, to afford monomers **1b** and **2b**.

Thanks to the presence of the bromine atom at the end of the oxyalkyl side chain, the subsequent precursor materials could be post-functionalizable and therefore suitable for the preparation of ionic materials, independently from the polymerization method adopted.

2.2 Preparation of precursor polymer: oxidative coupling with FeCl₃

Both the dye-sensitized precursor materials (**P1a-TPP** and **P2a-TPP**) were then obtained by oxidative coupling with iron chloride (FeCl₃) of monomers **1a** or **2a**, in presence of 3-[5-(4-phenoxy)-10,15,20-triphenylporphyrinyl]hexylthiophene (**T6OTPP**), and in the molar ratio of 4:1 (Scheme 1). In fact, to prevent self-aggregation phenomena typically observed for porphyrin derivatives, the TPP moiety was linked to the polymer but insulated from the polyconjugated thiophene backbone through a hexamethylene chain.

Despite this method is not regiospecific, as it leads to only partially regioregular materials (i.e., P1a-TPP), regioregular polyalkylthiophenes could be anyway obtained by using symmetrically substituted monomers or derivatives bearing aryl, thus sterically hindered, substituents in position 3. Moreover, this polymerization has several advantages such as a low cost of the oxidant, simplicity, and the possibility of obtaining the polymer in its more electrically conductive form.

2.3 Preparation of precursor polymer with Suzuki cross-coupling

This reaction is a cross-coupling between halides and boron derivatives that allows the formation of carbon-carbon bonds via a palladium-based catalytic cycle. Other possible coupling methods could be the Stille or Kumada reactions, but these methods involve highly toxic reagents (such as Bu₃SnCl or Ni(dppp)Cl₂) and unstable compounds (such as Grignard reagents). Suzuki coupling, on the other hand, requires milder reaction conditions and commercially available reagents, as well as the use of water as a co-solvent, and leads to a reduced formation of by-products that are not-toxic and easily removable.

The synthesized materials (**P1b-Bz** and **P2b-bz**) are therefore alternated *push-pull* polymers, made by oxyalkyl-substituted thiophene rings, that act as ED part, and benzothiadiazole units, that act as the EA component of the polymer. In fact, the term "push-pull" is derived from the fact that the electron-donating group "pushes" electrons to the electron-attracting group, which in turn "pulls" electrons away.³³

2.4 Preparation of post-functionalized polymers

All precursor polymers were then post-functionalized with tributyl phosphine, to obtain cationic polyelectrolytes as phosphonium salts (**P1a-buP**, **P2a-buP**, **P1b-buP** and **P2b-buP**). The decision to use this ionic moiety is due to their higher water/alcohol solubility, when compared to polymers with anionic groups found in the literature. In particular, the phosphines usually allow complete functionalization of the side substituents, thus giving a good solubility. In fact, all the final materials were found to be soluble in water, methanol, ethanol, *iso*- and, *n*-propanol.

Furthermore, an advantage of the post-functionalization with tributyl phosphine is the easy well-recovery of the polyelectrolyte, which precipitates in the reaction medium (i.e., toluene).³⁴

3. Characterization

3.1 Physical properties

The molecular weight of all precursor polymers, that are reported in Table 1, were determined by gel permeation chromatography (GPC) using THF as an eluent.

In the case of the dye-sensitized copolymers, the average-number molecular weights (M_n) obtained by iron trichloride method are substantially high. However, the degree of polymerization (X_n) for this class is less uniform, possibly due to the different content of oxygen in the polymer side chains.

In contrast, the materials obtained by the Suzuki cross-coupling present lower M_n values than the series discussed before, but a sufficient extent of conjugation length should be anyway guaranteed. Moreover, the X_n values for this polymerization are essentially similar and a better comparison of the properties can be evaluated.

Table 1. Physical properties of precursor polymers.

	<i>Reaction Yield (%)</i>	<i>Group Content (% mol)^[a]</i>	<i>M_n (KDa)</i>	<i>X_n^[b]</i>	<i>Đ^[d]</i>
<i>P0a-TPP</i>	45	80 Br, 20 TPP	33.6 ^[b]	94.7	1.7
<i>P1a-TPP</i>	71	79 Br, 21 TPP	12.2 ^[b]	32.7	1.3
<i>P2a-TPP</i>	78	75 Br, 25 TPP	19.5 ^[b]	36.9	1.3
<i>P0b-Bz</i>	77	100 Br	2.5 ^[b]	6.6	1.7
<i>P1b-Bz</i>	65	100 Br	2.5 ^[b]	6.3	1.3
<i>P2b-Bz</i>	54	100 Br	3.7 ^[b]	6.4	1.3
<i>P0a-buP</i>	91	80 buP, 20 TPP	47.9 ^[c]	94.7	1.7
<i>P1a-buP</i>	78	79 buP, 21 TPP	17.4 ^[c]	32.7	1.3
<i>P2a-buP</i>	89	75 buP, 25 TPP	28.5 ^[c]	36.9	1.3
<i>P0b-buP</i>	86	100 buP	3.8 ^[c]	6.6	1.7
<i>P1b-buP</i>	72	100 buP	3.8 ^[c]	6.3	1.3
<i>P2b-buP</i>	50	100 buP	5.7 ^[c]	6.4	1.3

[a] Determined by ¹H-NMR; [b] Determined by GPC relative to polystyrene standards; [c] Calculated from the average polymerization degree of the corresponding precursor polymers; [d] Polydispersity index, determined by GPC.

Since all the ionic copolymers were not soluble in the solvents commonly used for GPC (CHCl₃, THF and DMF), their weight can be anyway estimated since no structural changes in the macromolecular backbone are involved during the post-functionalization reaction with tributyl phosphine (Table 1).

3.2 NMR characterization

To confirm the identity and structure of the monomers and precursor copolymers, $^1\text{H-NMR}$ spectrometry analysis was carried out by dissolving the samples in deuterated chloroform (CDCl_3 , 7.26 ppm). However, the success of the post-functionalization reaction was verified by $^1\text{H-NMR}$ characterization in deuterated methanol (CD_3OD , 3.31 and 4.78 ppm), due to the change in solubility of the obtained products.

The obtainment of polymers (dye-sensitized copolymers) or materials with a sufficient extent of conjugation (push-pull copolymers) was confirmed by the occurrence of a general signal broadening, both in the aromatic and aliphatic regions. This phenomenon is due to the increased length of the macromolecular chains, which causes an increase of the relaxation time after the high-frequency pulse.

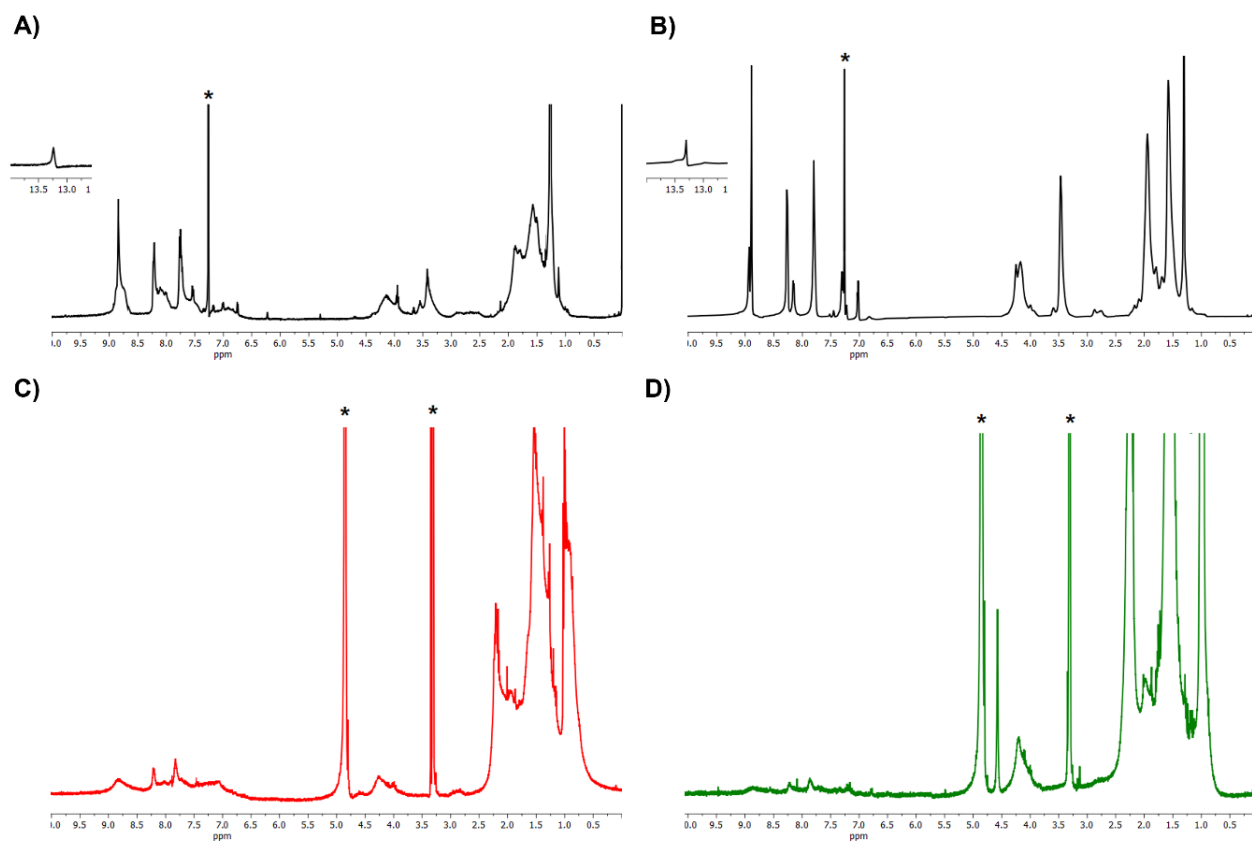


Figure 2. $^1\text{H-NMR}$ spectra of precursor (A: **P1a-TPP**; B: **P2a-TPP**) and ionic (C: **P1a-buP**; D: **P2a-buP**) dye-sensitized copolymers. Asterisk: solvent resonance.

In particular, for the dye sensitized copolymers (**P1a-TPP**, **P2a-TPP**) (Figure 2A and 2B), characteristic broad signals at 4.22-4.25 and 3.42-3.47 ppm for the CH_2OTTP and CH_2Br groups of the **T6OTTP** and **1a/2a** monomers, respectively, were displayed. Those signals, in addition to the

typical peaks relative to the TPP-porphyrin present in the aromatic region, confirmed their copolymerization and the retainment of the 4-phenoxy-triphenylporphyrin moiety in the side chains for both copolymers. Besides, the ratio of the integral peaks centered at ~ 4.20 and ~ 3.45 ppm made possible to quantify the final molar amount of the two monomers in the final materials (Table 1).

In the case of push pull materials, **P1b-Bz** and **P2b-Bz** (Figure 3A and 3B), two groups of multiplets in the aromatic region were observed at ~ 8.50 and 7.50 ppm, which are attributable to the benzothiadiazole and thiophene units. Indeed, although the M_n values (Table 1) resulted to be quite reduced, the enlarged peaks confirmed that polymerisation has taken place to some extent.

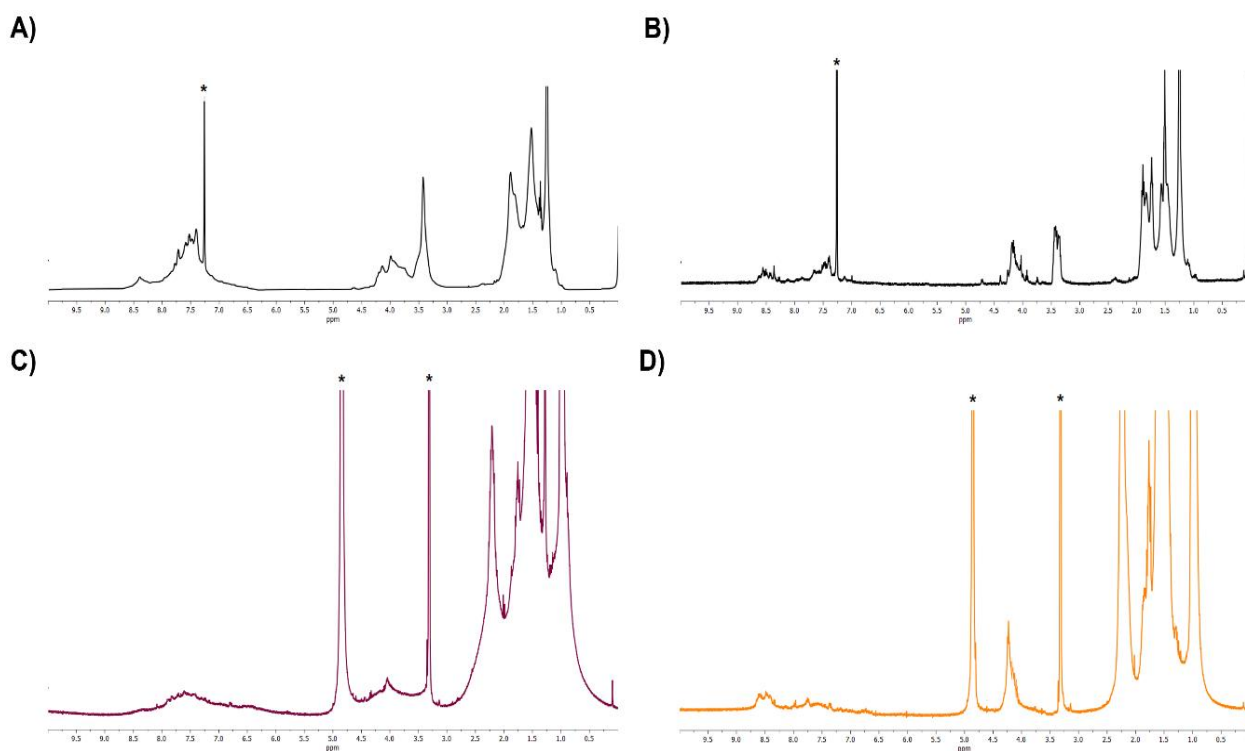


Figure 3. $^1\text{H-NMR}$ spectra of precursor (A: **P1b-Bz**; B: **P2b-Bz**) and ionic (C: **P1b-buP**; D: **P2b-buP**) push-pull copolymers. Asterisk: solvent resonance.

Finally, in addition to the disappearance of the peaks related to the CH_2Br protons (~ 3.45 ppm), the spectra of all ionic polymers (Figure 2C-2D and Figure 3C-3B) displayed signals centered at ~ 2.20 ppm related to the $\text{CH}_2\text{P}^+\text{bu}_3$ protons, thus indicating that the post-functionalization has occurred successfully and quantitatively. Moreover, for the dye sensitized copolymers the contents of porphyrin remained unaltered (Figure 2C-2D).

3.3 UV-Vis spectroscopy

To determine the optical properties of the synthesized materials, UV-Vis spectroscopic analyses were performed both in solution and in thin films, by recording the spectra in CHCl_3 (precursor derivatives) or water and in a wide range of different alcohols (ionic copolymers). In particular, due to their final application in OPVs, only the spectra in film obtained by drop-casting the polymer's solutions in ethanol onto quartz slides are reported here (Figure 4), taking the ethanol as a green reference solvent for the phosphonium salts (Table 2).

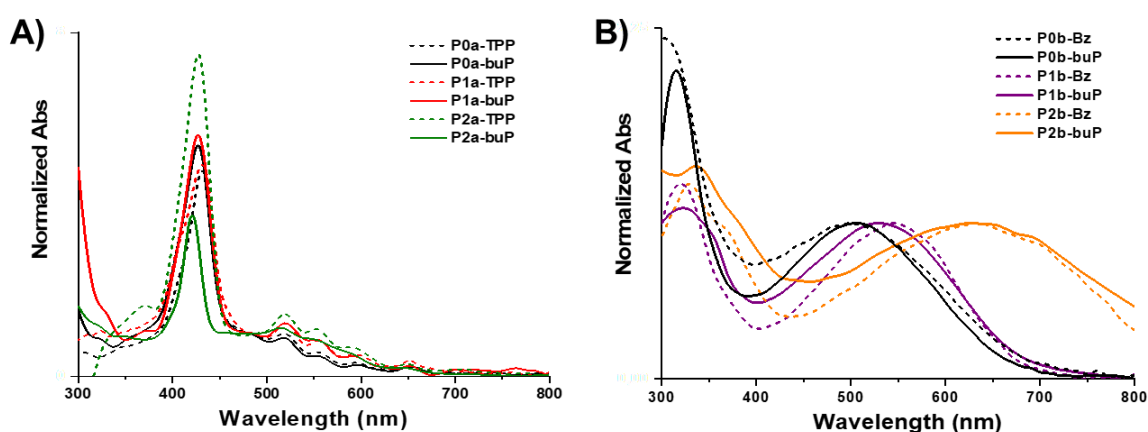


Figure 4. A) Normalized UV-Vis spectra in thin film of precursor (dashed line, CHCl_3) and ionic (solid line, EtOH) dye-sensitized materials; B) Normalized UV-Vis spectra in thin film of precursor (dashed line, CHCl_3) and ionic (solid line, EtOH) alternated D-A materials.

Table 2. Optical properties of post-functionalized copolymers.

Polymer	Film λ_{max} (nm)
P0a-buP	427, 483, (from 519 to 652),
P1a-buP	427, 485, (from 520 to 652)
P2a-buP	421, (from 514 to 646)
P0b-buP	315, 506
P1b-buP	322, 529
P2b-buP	337, 635

As expected, the copolymers containing the porphyrin group (**P0a-TPP**, **P1a-TPP**, **P2a-TPP**) show the typical *Soret* band, centered at 427 nm, and four *Q* bands at 520, 553, 591, and 650 nm (Figure 4A). In addition, a band related to the thiophene macromolecular chain is also visible at ~480 nm, for **P0a-TPP** and **P1a-TPP**. Whereas, for **P2a-TPP**, due to the increasing amount of oxygen atoms directly linked to the thiophene ring, this band is probably red shifted and thus partially overlapped

with the aforementioned Q bands of the porphyrin. Moreover, the comparison of the spectra of the aforementioned copolymers with those of the post-functionalized polymers (**P0a-buP**, **P1a-buP**, **P2a-buP**), shows slightly differences between the wavelengths of their absorption maxima, despite the insertion of sterically hindered groups in the side chain (phosphonium salts).

Polymers with alternating ED-EA structures (**P0b-Bz**, **P1b-Bz**, **P2b-Bz**) exhibit two main absorption bands in their spectra. While the first peak at shorter wavelengths (~ 320 nm) is due to $\pi \rightarrow \pi^*$ electronic transitions of the donor-conjugate system, that at longer wavelengths (~ 550) nm is caused by the $\pi \rightarrow \pi^*$ transition of the donor-acceptor charge-transfer complex (Figure 4B).

Furthermore, the presence of the oxygen atom directly linked to the aromatic ring can inject more charge to the system, thus stabilizing the macromolecular chain and leading to a further reduction of the HOMO-LUMO band gap of the material, resulting in an absorption of radiation at lower energy. In fact, by increasing the number of oxygens in the side chains, a strong red shift of the maximum absorption is obtained passing from **P0b-Bz** to **P2b-Bz**.

Also for this series of copolymers (**P0b-buP**, **P1b-buP**, **P2b-buP**), the optical behaviour does not show any significant changes after the post-functionalization reaction.

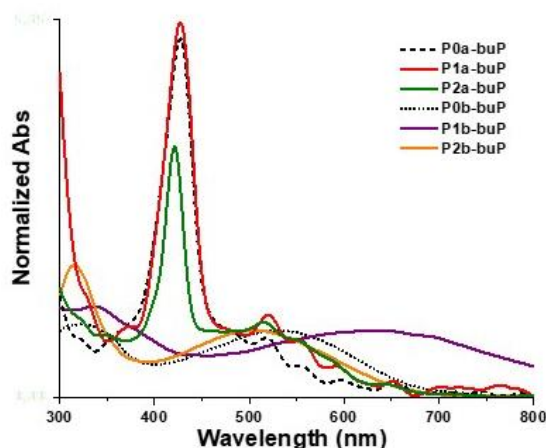


Figure 5. Normalized UV-Vis spectra in thin film of all synthesized ionic derivatives.

3.4 Electrochemical properties

With the aim to test the prepared ionic materials as cathode interlayers (CTLs) in halogen free BHJ OPVs, their redox behavior has been also investigated by cyclic voltammetry analyses (CVs) in thin films.

The energies of the HOMO/LUMO levels were then calculated and compared with those of an alcohol-soluble blend of poly{3-[6-(tributyl-phosphonium)-hexyl]-thiophene-2,5-diyl bromide} (**PT6buP**) and malonodiserinolamide fullerene (**C₆₀-Ser**), previously synthesized by the research group, which will be tested as photoactive layer.

For the push-pull derivatives (**P1b-buP** and **P2b-buP**) both the HOMO and LUMO energy levels were evaluated by CVs, according to the following equation:

$$\text{HOMO (eV)} = -e (E_{\text{ox}} + 4.24)$$

$$\text{LUMO (eV)} = -e (E_{\text{red}} + 4.24)$$

where 4.24 eV is the saturated calomel electrode (SCE) absolute potential.

On the other hand, in the case of the dye-sensitized copolymers (**P1a-buP** and **P2a-buP**), the LUMO levels were estimated indirectly since the reduction potentials were outside the electrochemical stability window of the electrolyte. These energy levels were then calculated from the HOMO levels and the optical bandgaps ($E_{\text{g}}^{\text{Opt}}$), obtained from the UV-Vis spectra of the films (Figure 5), with the equation:

$$\text{LUMO (eV)} = \text{HOMO} + E_{\text{g}}^{\text{Opt}}$$

The values obtained are listed in Table 3.

Table 3. Redox potentials, HOMO/LUMO level energies and polymers energy gap.

	$E_{\text{onset}}^{\text{ox}}$ (V vs SCE)	$E_{\text{onset}}^{\text{red}}$ (V vs SCE)	HOMO (eV)	LUMO (eV)	E_{g} (eV)
P0a-buP	0.84	-	-5.08	-2.85	2.23 ^[a]
P1a-buP	0.57	-	-4.81	-2.63	2.18 ^[a]
P2a-buP	0.59	-	-4.83	-2.77	2.06 ^[a]
P0b-buP	1.04	-1.01	-5.28	-3.23	2.03 ^[b]
P1b-buP	0.56	-0.96	-4.80	-3.28	1.52 ^[b]
P2b-buP	0.50	-0.84	-4.74	-3.40	1.34 ^[b]

[a] Optical band gap, $E_{\text{g}}^{\text{Opt}}$; [b]; Electrochemical band gap, $E_{\text{g}}^{\text{Elect}}$.

Firstly, for both the studied polymeric series, it is possible to determine the conjugative effect of the oxygen atoms linked to the thiophene ring. In fact, lower oxidation potentials as well as strongly reduced band gaps were displayed when the content of oxygen increases and this is particularly true for the dioxy-alkyl push-pull material **P2b-buP** (Table 3).

Then, an optimal cascade energy level alignment with the binary photoactive blend (**PT6buP:C₆₀-Ser**, Figure 6) was obtained. Therefore, all the prepared copolymers could be employed as cathode interlayers due to their cationic nature and fine matching with the work functions of anode and cathode.

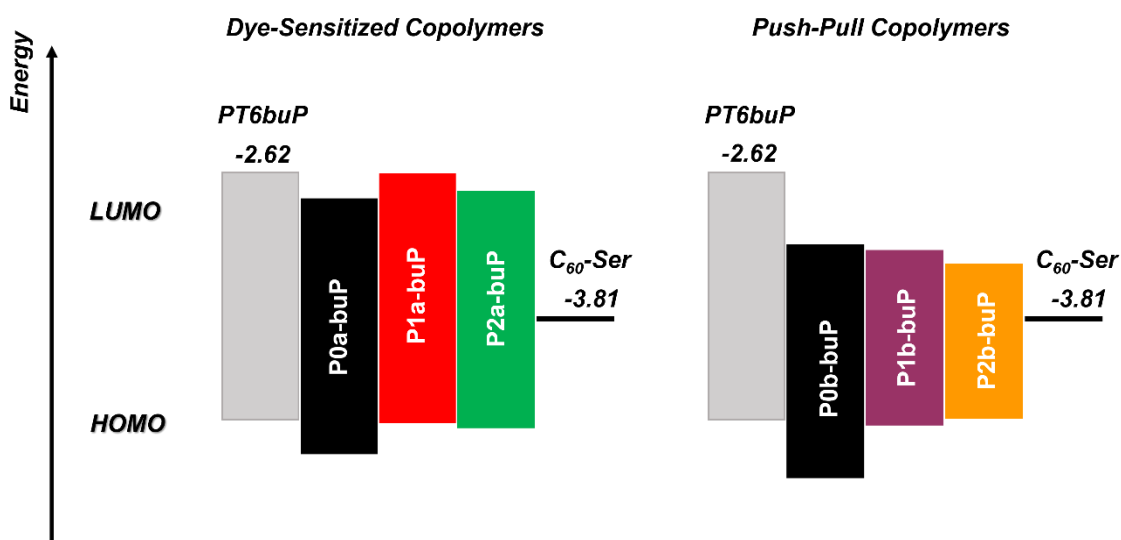


Figura 6. HOMO/LUMO levels of synthesized copolymers, compared to the other two main components of an organic solar cell.

3.5 Organic solar cells

As previously stated, the synthesized ionic materials were finally tested as CTLs in halogen free BHJ solar cells having the standard geometry: ITO//anode interlayer (ATL, PEDOT:PSS)/photoactive layer (PT6buP:C₆₀-Ser)/CTLs//Al.

Table 4 shows the main electrical parameters of the prepared devices, obtained by depositing the ionic materials from ethanol solutions. For comparison, the results obtained in the absence of a cathode interlayer and in the presence of a commercial one, (poly[9,9-bis(3'-(N,N-dimethyl)-N-ethylammonium-propyl-2,7-fluorene-alt-2,7-(9,9-dioctylfluorene))dibromide] (**PFN-Br**), are also listed.

Table 4. Properties of BHJ OSCs prepared with alcohol-soluble materials as CTLs (average values collected from 5 devices).

	J_{sc} (mA·cm ⁻²) ^[a]	V_{oc} (V) ^[b]	FF ^[c]	PCE (%) ^[d]
PT6buP:C₆₀-Ser	8.81	0.57	0.56	2.81
PT6buP:C₆₀-Ser//PFN-Br	11.70	0.61	0.58	4.15
PT6buP:C₆₀-Ser//P0a-buP	9.90	0.59	0.59	3.45
PT6buP:C₆₀-Ser//P1a-buP	10.41	0.58	0.59	3.56
PT6buP:C₆₀-Ser//P2a-buP	11.30	0.58	0.59	3.87
PT6buP:C₆₀-Ser//P0b-buP	9.90	0.58	0.58	3.33
PT6buP:C₆₀-Ser//P1b-buP	10.95	0.59	0.57	3.68
PT6buP:C₆₀-Ser//P2b-buP	12.20	0.60	0.59	4.32

[a] Short circuit current; [b] Open circuit voltage; [c] Fill factor; [d] Photoconversion efficiency.

The efficiency of a solar cell (PCE) is calculated from the parameters shown in Table 4, obtained by the current density (mA/cm²) versus voltage (Volts) curves. In details:

- J_{sc} : short circuit current density, i.e., the maximum current generated by the cell under illumination, thus when the voltage is zero;
- V_{oc} : open-circuit voltage, i.e., the maximum voltage applied to the cell when the output current is zero;
- FF: fill factor, which takes in account the non-ideality of the device and it can be calculated with the formula:

$$FF = \frac{J_{MP} * V_{MP}}{J_{SC} * V_{OC}}$$

Where J_{MP} and V_{MP} are the current density and voltage at the point of maximum power.

- PCE: power conversion efficiency, thus the ratio between the maximum power generated by the cell (P_{max}) and the incident radiant power (P_{inc}).

$$PCE = \frac{P_{max}}{P_{inc}} * 100 = \frac{V_{OC} * J_{SC} * FF}{P_{inc}}$$

The obtained results show that all the synthesized ionic materials lead to interesting and promising PCE values, confirming an increase in the final efficiency when the prepared polymers are used as cathode interlayers.

In particular, mostly of them show an increase of 30% in the PCE value if compared with a cell devoid of interlayer. Indeed, thanks to the use of interlayers it is possible to extend the coverage of the UV-Vis absorption spectra of the photoactive layers (Figure 7). Moreover, when **P2b-buP** is used, comparable and even better parameters of those obtained by using commercial PFN-Br were displayed, with a final PCE increase of 50%.

This opens the way for further deposition tests, may be from other green solvents, or under different conditions to optimise the final device.

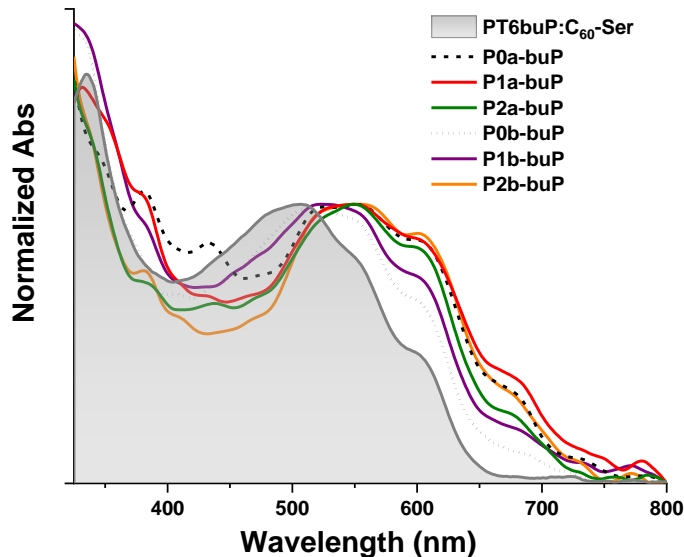


Figure7. Normalized UV-Vis spectra in thin films of photoactive layer (PT6buP:C₆₀-Ser), alone or in presence of the synthesized ionic materials used as cathode interlayers.

Conclusion

In the present work, oxyalkyl-thiophene monomers were prepared and copolymerized in presence of 3-[5-(4-phenoxy)-10,15,20-triphenylporphyrinyl]hexylthiophene or 2,1,3-benzothiadiazole-4,7-bis(boronic acid pinacol ester), to afford two classes of materials. In particular, the dye-sensitized polymers (**P1a-TPP** and **P2a-TPP**) and push-pull derivatives (**P1b-Bz** and **P2b-Bz**) were obtained by oxidative polymerization and Suzuki cross-coupling reaction, respectively.

The precursor copolymers were then subjected to a post-functionalization reaction with tributyl phosphine to obtain completely ionic products (phosphonium salts, **P1a/b-buP** and **P2a/b-buP**), which resulted to be soluble in many green solvents such as alcohols or water.

While all their structures were confirmed by ¹H-NMR spectroscopy, the molecular weights were determined by GPC analysis, resulting in acceptable values to give filmable materials.

Then a deep study of the optical properties, both in solution and in thin film, was performed. The effect of the insertion of an oxygen atom directly linked to the thiophene ring was evidenced, the behavior of the tetraphenyl-porphyrin group in the side chain was investigated and the obtainment of polymers with small band-gap (push-pull) was confirmed.

After electrochemical characterization by CVs and subsequent determination of the energy level alignment, the ionic polymers were finally tested as cathode interlayers in halogen-free BHJ OSCs, displaying the best results when **P2b-buP** was used. The obtained findings are encouraging, although further optimization of the cell preparation method is needed.

Experimental Part

1. Materials and Methods

Anhydrous chloroform (CHCl_3): the commercially available Honeywell product, after stirring under reflux for a couple of hours with the anhydrating agent P_2O_5 , was distilled in argon flow and stored on molecular sieves.

Anhydrous toluene (C_7H_8): the commercially available Sigma-Aldrich product was distilled in the presence of metallic Na/K alloy and benzophenone as indicator, over molecular sieves in an inert atmosphere.

3-Methoxythiophene, 98% w/w (**1**), 3,4-dimethoxythiophene, 97% w/w (**2**), 2,1,3-benzothiadiazole-4,7-bis(boronic acid pinacol ester), 95% w/w (**Bz**) and poly[9,9-bis(3'-(N,N-dimethyl)-N-ethylammonium-propyl-2,7-fluorene)-alt-2,7-(9,9-dioctylfluorene)]dibromide (**PFN-Br**) are commercially available (Sigma Aldrich).

6-Bromo-hexanol (**B6OH**), 3-[5-(4-phenoxy)-10,15, 20-triphenylporphyrinyl]hexylthiophene (**T6OTPP**), poly{3-(6-tributylphosphoniumhexyl)thiophene-co-3-[5-(4-phenoxy)-10,15,20-triphenylporphyrinyl]hexylthiophene bromide} (**P0a-buP**), poly4-[3-(6-tributylphosphoniumhexyl)thiophen-2-yl]benzo[c][1,2,5]thiadiazole (**P0b-buP**), poly{3-[6-tributylphosphonium)-hexyl]-thiophene-2,5-diyl bromide} (**PT6buP**) and malonodiserinamide fullerene (**C60-Ser**) were previously prepared and characterized by the research group.

Diethyl ether (Et_2O) and tetrahydrofuran (THF) were freshly distilled before use to remove the stabilizer. All manipulations involving air- or moisture-sensitive reagents were performed under inert atmosphere in flame-dried glassware.

2. Instruments

The ^1H -NMR spectra of the monomers, precursor and post-functionalised polymers were recorded at room temperature using a Varian Mercury spectrometer operating at 400 MHz, in CDCl_3 or CD_3OD solutions. Chemical shifts are given in ppm and were determined relative to the resonance shift of the solvent.

The molecular weight of the precursor polymers was determined in THF by gel permeation chromatography (GPC) using a LAb Flow 2000 HPLC pump, a Rheodyne 7725i injector, a Phenomenex Phenogel Mixed 5μ MXL column and a KNAUER RI K-2301 detector. The calibration curve was performed using standard monodisperse polystyrene samples.

The UV-Vis absorption spectra were recorded with the Perkin Elmer Lambda 20 apparatus, using 1 cm quartz cuvettes and preparing the samples in CHCl_3 or alcohols and H_2O (10^{-5} M polymer solutions). Thin-film measurements were made on polymer samples on quartz slides obtained by spray-coating deposition.

The FT-IR spectra were recorded on a KBr disk using a Perkin Elmer Spectrum One FT-IR spectrophotometer interfaced with a data processor.

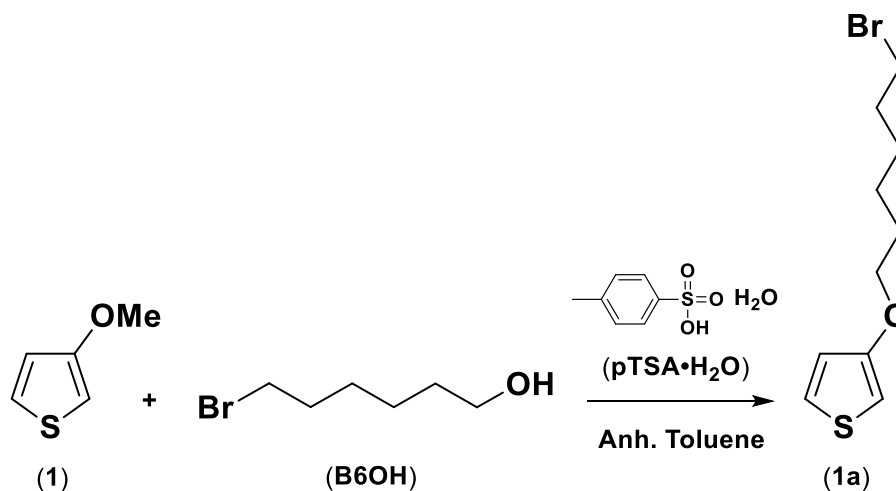
Cyclic voltammetries (CVs) were performed at room temperature in a three-compartment glass cell under Ar pressure by using an AMEL 5000 Electrochemical System. Ionic polymers were deposited by drop-casting from methanol on a 1 mm-diameter Pt electrode. The auxiliary electrode was Pt wire spiral, and the reference electrode was aqueous saturated calomel electrode (SCE). Supporting electrolyte was $0.1 \text{ mol L}^{-1} (\text{C}_4\text{H}_9)_4\text{NClO}_4$, while solvent was selected in order to avoid the dissolution of cast films: mixture of 25% CH_3CN and 75% toluene ($E^\circ_{[\text{FC}^+/\text{FC}]} = 0.599 \text{ V vs. SCE}$, absolute potential of FC^+/FC is assumed 4.84 eV).

The deposition of the aluminium cathode on the photovoltaic cells was carried out with the aid of an Edward Coating System E306A spin coating equipment, reaching pressures of 10^{-6} millibars. The evaluation of the performance of the manufactured photovoltaic cells was carried out using a Keithley 2400 multimeter (Solar Simulator).

3. Synthesis

Synthesis of monomers: transesterification reaction

3-(6-Bromohexyloxy)thiophene (1a)



<i>Reagents/Solvents</i>	<i>Molar ratio</i>	<i>Numbers of moles (mmol)</i>	<i>Mw (g/mol)</i>	<i>Quantity</i>
1	1.0	4.52	114.16	0.510 g
B6OH	1.5	6.57	181.07	1.190 g
pTSA·H ₂ O	0.1	0.45	190.22	0.083 g
Anh. toluene				15.0 mL

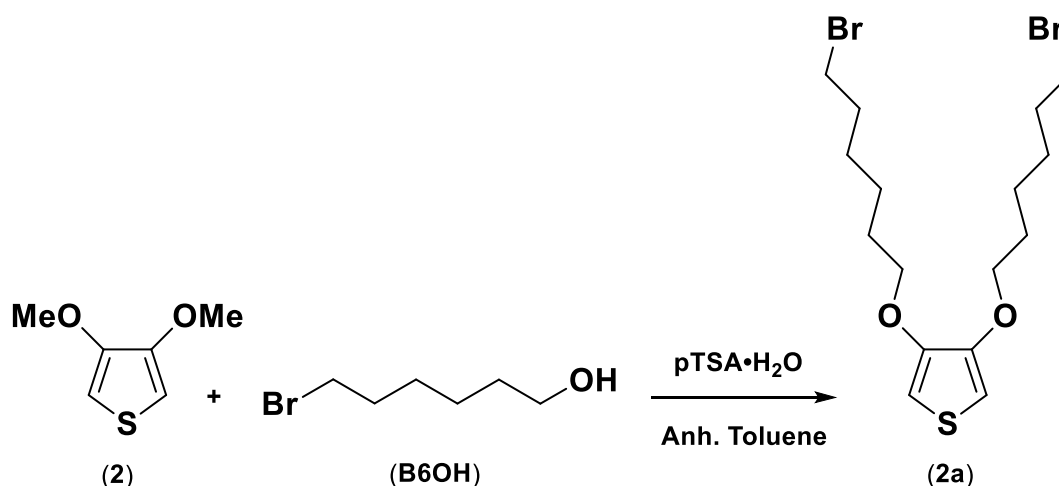
In a three-neck round bottom flask, 1.190 g of B6OH (6.57 mmol) and a catalytic amount of *p*-toluenesulfonic acid monohydrate (pTSA·H₂O, 0.45 mmol) were added under stirring to a solution of 3-methoxythiophene (4.52 mmol) in dry toluene (15.0 mL). The mixture was refluxed for 24h under nitrogen atmosphere.

Afterwards, the system was brought to room temperature and the reaction solvent removed under reduced pressure. The crude product was then recovered with 60.0 mL of CH₂Cl₂ and transferred to a separating funnel, where the organic phase was subsequently washed with 50.0 mL of a saturated NaHCO₃ solution and half-saturated NaCl solution (4 x 80.0 mL), up to neutrality. The organic phase was dried over anh. Na₂SO₄ and filtered through a pleated filter. After removal of the solvent under reduced pressure, the crude product was finally purified by a chromatographic column (SiO₂; hexane/ethyl acetate 85:15) to give 0.988 g of 3-(6-bromohexyloxy)thiophene (**1a**) as yellow oil (83% yield).

δ ^1H (400 MHz, CDCl_3 , ppm): 7.17 (dd, 1H, Th H5), 6.75 (dd, 1H, Th H4), 6.23 (dd, 1H, Th H2), 3.95 (t, 2H, ThOCH_2), 3.42 (t, 2H, CH_2Br), 1.89 (m, 2H, $\text{ThOCH}_2\text{CH}_2$), 1.79 (m, 2H, $\text{CH}_2\text{CH}_2\text{Br}$), 1.50 (m, 4H, $(\text{CH}_2)_2$).

δ ^{13}C (400 MHz, CDCl_3 , ppm): 158.50 (Th C3), 125.26 (Th C5), 120.15 (Th C4), 97.72 (Th C2), 70.62 (ThOCH_2), 34.45 (CH_2Br), 33.33 ($\text{CH}_2\text{CH}_2\text{Br}$), 29.75 ($\text{ThOCH}_2\text{CH}_2$), 28.58, 25.97 ($(\text{CH}_2)_2$).

3,4-(6,6'-Dibromohexyloxy)thiophene (**2a**)



Reagents/Solvents	Molar ratio	Numbers of moles (mmol)	Mw (g/mol)	Quantity
2	1.0	3.40	144.19	0.500 g
B6OH	1.5	10.19	181.07	1.866 g
pTSA·H ₂ O	0.1	0.34	190.22	0.065 g
Anh. toluene				80.0 mL

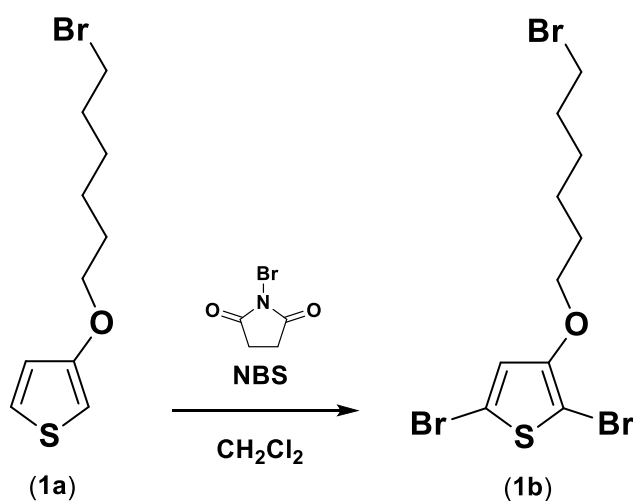
The same procedure described for **1a** was followed starting from 3,4-dimethoxythiophene (0.500 g, 3.40 mmol) in dry toluene (80.0 mL), with B6OH (1.846 g, 10.19 mmol) and pTSA·H₂O (0.065 g, 0.34 mmol), to obtain 0.917 g of 3,4-(6,6'-bibromohexyloxy)thiophene (**2a**) as yellow-greenish oil (61% yield).

δ ^1H (400 MHz, CDCl_3 , ppm): 6.17 (s, 2H, Th H2), 3.98 (t, 4H, ThOCH_2), 3.41 (t, 4H, CH_2Br), 1.89 (m, 4H, $\text{ThOCH}_2\text{CH}_2$), 1.83 (m, 4H, $\text{CH}_2\text{CH}_2\text{Br}$), 1.50 (m, 8H, $(\text{CH}_2)_2$).

δ ^{13}C (400 MHz, CDCl_3 , ppm): 147.39 (Th C3), 97.00 (Th C2), 70.25 (ThOCH_2), 33.76 (CH_2Br), 32.66, 28.83, 27.88, 25.22 ($(\text{CH}_2)_n$).

Synthesis of monomers: dibromination reaction

2,5-Dibromo-3-(6-bromohexyloxy)thiophene (**1b**)



Reagents/Solvents	Molar ratio	Numbers of moles (mmol)	Mw (g/mol)	Quantity
1a	1.0	0.76	263.19	0.200 g
NBS	2.2	1.67	177.98	0.298 g
CH_2Cl_2				5.0 mL

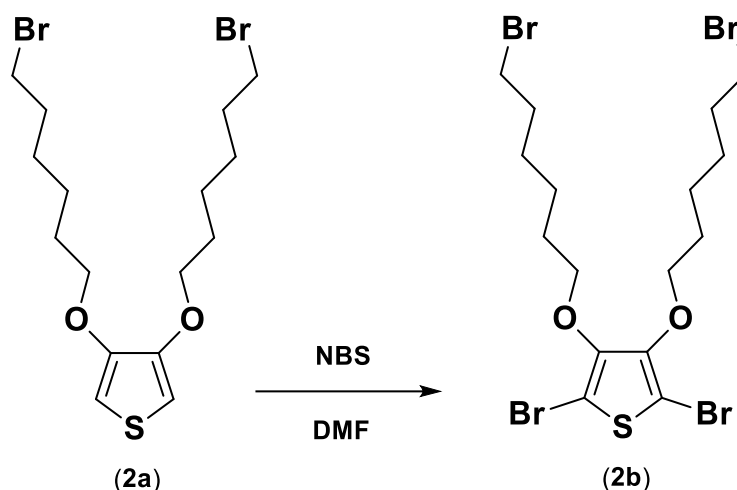
To a solution of **1a** (0.76 mmol) in CH_2Cl_2 (5.0 mL), 0.298 g of N-bromosuccinimide (NBS) were added portion wise. After addition completed, the solution was left under stirring, at room temperature, and protected by light for 21h. When the reaction time passed, the crude product was diluted with CH_2Cl_2 (60.0 mL) and subsequently washed with 60.0 mL of saturated NaHCO_3 solution and half-saturated NaCl solution (2 x 100 mL), up to neutrality. The organic phase was anhydriified with Na_2SO_4 , filtered and concentrated under reduced pressure.

Finally a chromatographic column (SiO_2 ; cyclohexane/ CH_2Cl_2 90:10) was carried out on the crude product, to obtain 0.255 g of 2,5-dibromo-3-(6-bromohexyloxy)thiophene (**1b**) as a light-yellow oil (80% yield).

δ ^1H (400 MHz, CDCl_3 , ppm): 6.76 (s, 1H, Th H4), 4.00 (t, 2H, ThOCH₂), 3.42 (t, 2H, CH₂Br), 1.90 (m, 2H, ThOCH₂CH₂), 1.75 (m, 2H, CH₂CH₂Br), 1.50 (m, 4H, (CH₂)₂).

δ ^{13}C (400 MHz, CDCl_3 , ppm): 153.89 (Th C3), 121.01 (Th C4), 109.86 (Th C5), 90.88 (Th C2), 72.45 (ThOCH₂), 33.88 (CH₂Br), 32.78 (CH₂CH₂Br), 29.34 (ThOCH₂CH₂), 27.96, 25.17 ((CH₂)₂).

2,5-Dibromo-3,4-(6,6'-dibromohexyloxy)thiophene (**2b**)



Reagents/Solvents	Molar ratio	Numbers of moles (mmol)	Mw (g/mol)	Quantity
2a	1.0	0.45	442.25	0.200 g
NBS	2.5	1.13	177.98	0.202 g
DMF				6.0 mL

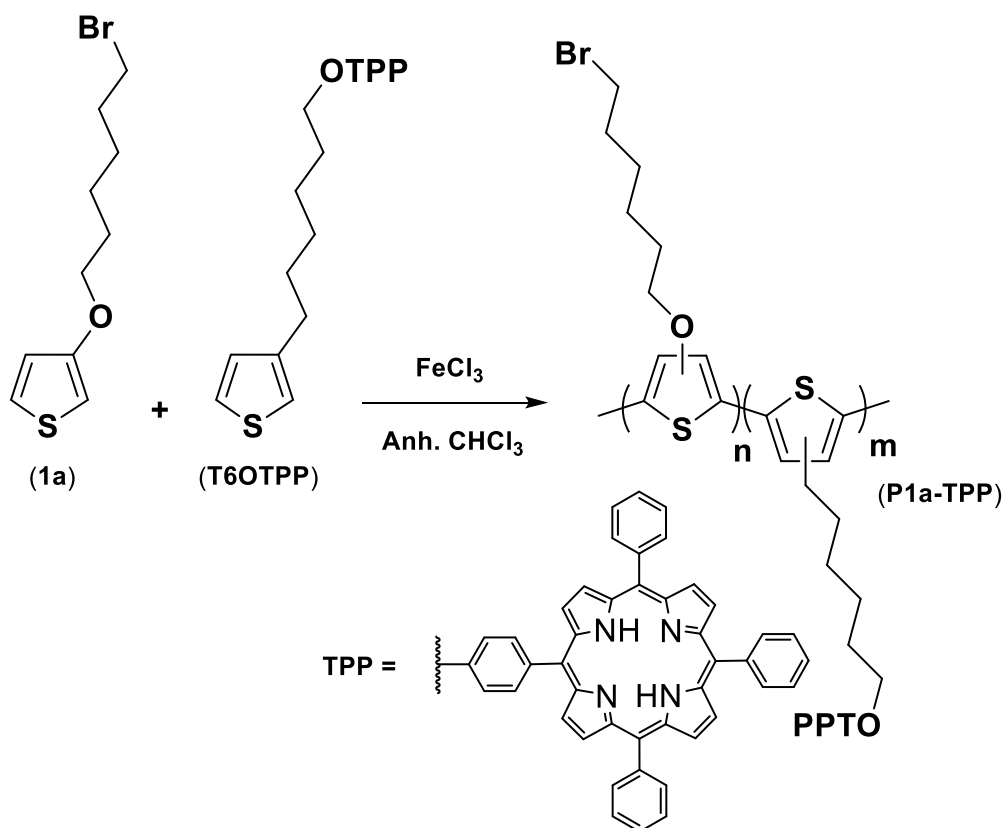
In a three-neck flask and under N₂ flow, 0.200 g of 2a were dissolved in 2.0 ml of dimethylformamide (DMF). A solution of NBS (1.13 mmol) in DMF (4.0 mL) was slowly added via a dropping funnel, resulting in a red-orange solution. Under light protection, the system was allowed to react for 24 hours at room temperature with constant stirring. The reaction mixture was then transferred to a separating funnel containing 40 ml of a saturated KHCO₃ solution, extracted with ethyl acetate (3 x 40.0 mL) and finally neutralized with a half-saturated solution of NaCl. After dehydration and concentration at rotavapor, purification is carried out by chromatographic column (SiO₂; cyclohexane/ethyl acetate 85:15) obtaining 0.202 g of 2,5-dibromo-3,4-(6,6'-dibromohexyloxy)thiophene (**2b**) as a red oil (75% yield).

δ ¹H (400 MHz, CDCl₃, ppm): 4.06 (t, 4H, ThOCH₂), 3.42 (t, 4H, CH₂Br), 1.89 (m, 4H, ThOCH₂CH₂), 1.74 (m, 4H, CH₂CH₂Br), 1.52 (m, 8H, (CH₂)₂).

δ ¹³C (400 MHz, CDCl₃, ppm): 147.45 (Th C3), 95.40 (Th C2), 73.64 (ThOCH₂), 33.74 (CH₂Br), 32.68, 29.72, 27.88, 25.08 ((CH₂)_n).

Synthesis of precursor polymers: oxydative coupling with FeCl₃

Poly{3-(6-bromohexyloxy)thiophene-co-3-[5-(4-phenoxy)-10,15,20-triphenylporphyrinyl]hexylthiophene} (P1a-TPP)



Reagents/Solvents	Molar ratio	Numbers of moles (mmol)	Mw (g/mol)	Quantity
1a	4.0	0.57	263.19	0.150 g
T6OTPP	1.0	0.14	790.03	0.114 g
FeCl ₃	20.0	2.84	162.20	0.461 g
Anh. CHCl ₃				10.0 mL
CH ₃ NO ₂				3.0 mL

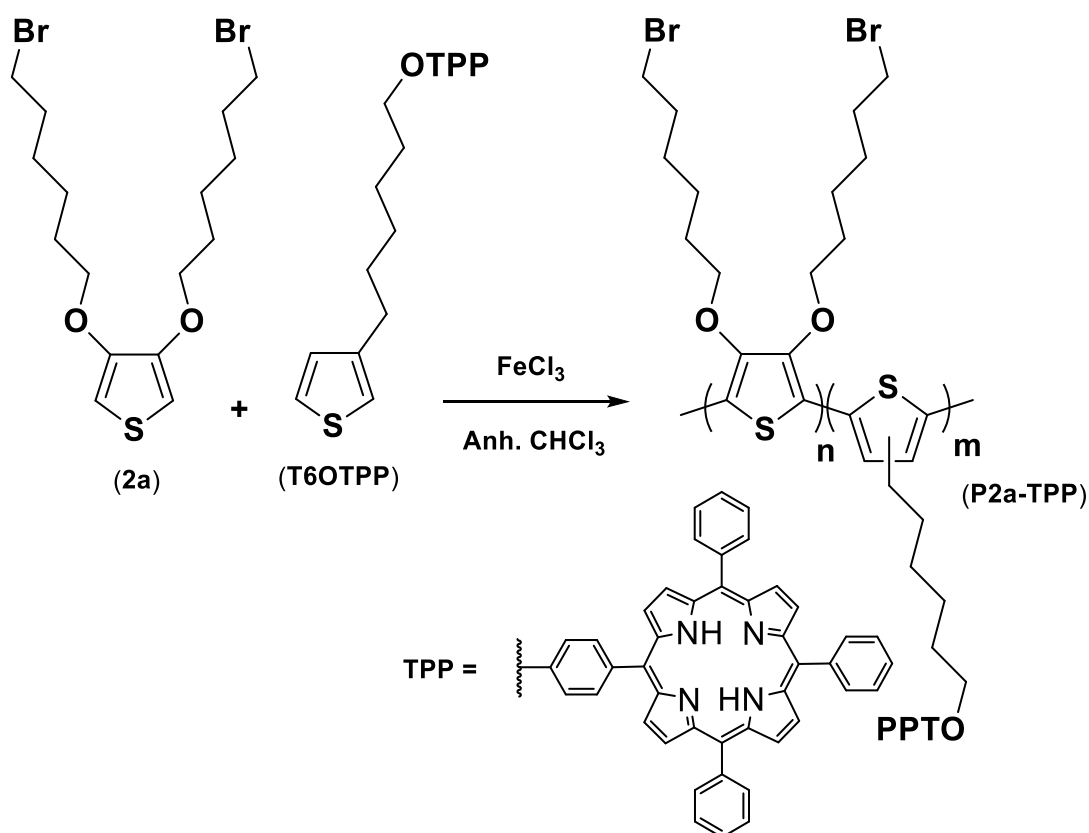
Anhydrous ferric trichloride (FeCl₃, 2.84 mmol) was dissolved in nitromethane (CH₃NO₂, 3.0 mL) and added dropwise to a three-necked round bottom flask, containing a solution of 1a (0.57 mmol) and T6OTPP (0.14 mmol) in dry CHCl₃ (10.0 mL). The reaction mixture was left to react for 50 minutes, under a flow of nitrogen saturated with anhydrous chloroform, before freshly distilled THF (10 mL) was added and left under stirring for another 40 minutes. The mixture was then transferred to a separating funnel, diluted with CHCl₃ and subsequently washed with 2% aq. HCl and with water until neutrality. To check the exhaustive extraction of iron (III), an assay with 5% aq. NH₄SCN was

taken on the aqueous phase at each extraction. The collected organic phase was dried over Na_2SO_4 , filtered, concentrated under reduced pressure and finally precipitated in MeOH. The precipitated polymer was decanted, filtered on Teflon membrane (porosity: $0.45\ \mu\text{m}$), and washed with plenty of CH_3OH , recovering 0.189 g of poly{3-(6-bromohexyloxy)thiophene-co-3-[5-(4-phenoxy)-10,15,20-triphenylporphyrinyl]hexylthiophene} (**P1a-TPP**) as purple solid (71% yield).

$\delta\ ^1\text{H}$ (400 MHz, CDCl_3 , ppm): 13.24 (br s, 2H, NH), 8.84 (br s, 8H, Pyrrolic-H), 8.21 (br s, 4H, Ar-H), 8.10 (br s, 4H, Ar-H), 7.75 (br s, 5H, Ar-H), 7.52 (br m, 4H, Ar-H), 7.17-6.70 (br m, 4H, Ar-H and Th-H), 4.22 (br t, 2H, CH_2OTPP), 4.12 (br t, 2H, ThOCH_2), 3.42 (br t, 2H, CH_2Br), 2.88 (br m, 2H, ThCH_2), 1.89 (br m, 6H, $(\text{CH}_2)_n$), 1.56 (br m, 10H, $(\text{CH}_2)_n$).

FT-IR (KBr, cm^{-1}): 3318, 2919, 2850, 1723, 1600, 1508, 1471, 1440, 1402, 1351, 1246, 1176, 1072, 1002, 981, 966, 802, 732, 732, 702, 647, 527.

{3,4-(6'-6-dibromohexyloxy)thiophene-co-3-[5-(4-phenoxy)-10,15,20-triphenylporphyrinyl]hexylthiophene} (**P2a-TPP**)



<i>Reagents/Solvents</i>	<i>Molar ratio</i>	<i>Numbers of moles (mmol)</i>	<i>Mw (g/mol)</i>	<i>Quantity</i>
2a	4.0	0.34	442.25	0.150 g
T6OTPP	1.0	0.08	798.03	0.068 g
FeCl ₃	20.0	1.69	162.20	0.275 g
Anh. CHCl ₃				9.0 mL
CH ₃ NO ₂				2.0 mL

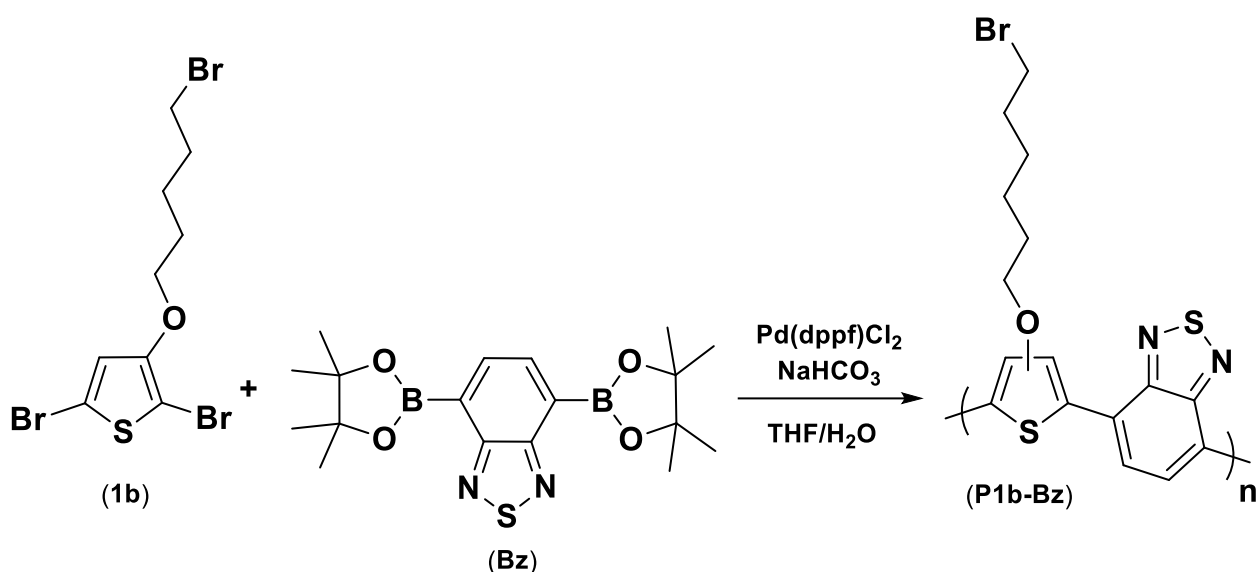
The same procedure described for P1a-TPP was followed starting from 2a (0.150 g, 0.34 mmol), T6OTPP (0.068 g, 0.08 mmol) and FeCl₃ (0.275 g, 1.36 mmol), to obtain 0.140 g of poly{3,4-(6'6'-dibromohexyloxy)thiophene-co-3-[5-(4-phenoxy)-10,15,20-triphenylporphyrinyl]hexylthiophene} (**P2a-TPP**) as purple solid (78% yield).

δ ¹H (400 MHz, CDCl₃, ppm): 13.30 (br s, 2H, NH), 8.93 and 8.89 (br m and br s, 8H, Pyrrolic-H), 8.27 (br m, 6H, Ar-H), 8.16 (br m, 2H, Ar-H), 7.80 (br m, 9H, Ar-H), 7.30 (br m, 2H, Ar-H), 7.02 (br s, 1H, Th-H), 4.25 (br t, 2H, CH₂OTPP), 4.17 (br t, 2H, ThOCH₂), 3.47 (br t, 2H, CH₂Br), 2.76 (br m, 2H, ThCH₂), 1.94 (br m, (CH₂)_n), 1.58 (br m, (CH₂)_n).

FT-IR (KBr, cm⁻¹): 3318, 2932, 2851, 1726, 1662, 1605, 1511, 1471, 1439, 1370, 1284, 1246, 1175, 1072, 1002, 966, 844, 802, 752, 702, 647, 527.

Synthesis of precursor polymer: Suzuki cross-coupling reaction

Poly4-[3-(6-bromohexyloxy)thiophen-2-yl]benzo[c][1,2,5]thiadiazole (**P1b-Bz**)



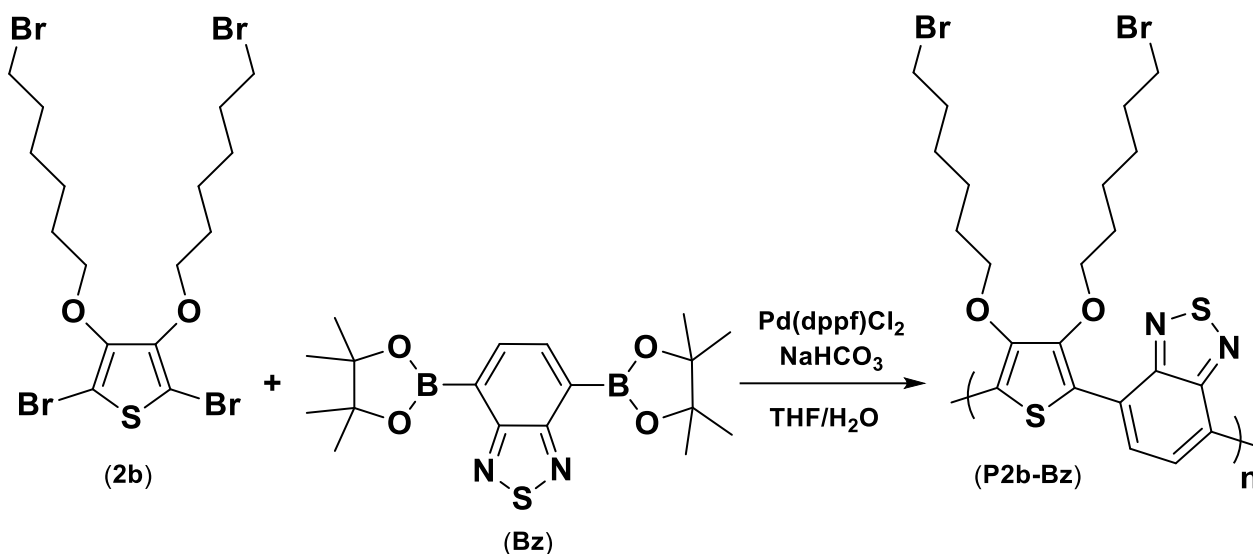
Reagents/Solvents	Molar ratio	Numbers of moles (mmol)	Mw (g/mol)	Quantity
1b	1.0	0.28	420.99	0.120 g
Bz	1.0	0.28	388.10	0.111 g
NaHCO ₃	5.0	1.42	84.00	0.120 g
Pd(dppf)Cl ₂	0.1	0.03	816.00	0.023 g
THF				4.0 mL
H ₂ O				2.0 mL

In a three-necked round bottom flask equipped with a condenser, a mixture of 1b (0.28 mmol), pinacolic acid ester of 2,1,3-benzothiadiazole-4,7-bis(boronic) (Bz, 0.28 mmol), Pd(dppf)Cl₂ (0.03 mmol) and NaHCO₃ in 2.0 mL of H₂O and 4.0 mL of THF was heated to 85°C and kept under stirring for 3h. After cooling to room temperature, the reaction mixture was diluted with 100.0 mL of CHCl₃ and washed with half-saturated aqueous NaCl solution (3 x 100.0 mL). The organic phase was anhydriified over Na₂SO₄, filtered and then concentrated, before precipitation in MeOH. The obtained polymer was recovered by filtration on Teflon membrane and thoroughly washed with CH₃OH, acetone and lastly diethyl ether, to afford 0.079 g of poly-[3-(6-bromohexyloxy)thiophen-2-yl]benzo[c][1,2,5]thiadiazole (**P1b-Bz**) as blue solid (65% yield).

δ ¹H (400 MHz, CDCl₃, ppm): 8.39 (br m, Bz-H), 8.07-6.98 (br m, Th-H4, terminal Bz-H and terminal Th-H), 4.12-3.98 (br m, ThOCH₂), 3.43 (br t, CH₂Br), 1.89, 1.52 and 1.26 (br m, (CH₂)_n).

FT-IR (KBr, cm⁻¹): 2920, 2850, 1723, 1534, 1482, 1436, 1382, 1199, 1088, 826, 750, 644, 527.

Poly4-[3,4-(6,6'-dibromohexyloxy)thiophen-2-yl]benzo[c][1,2,5]thiadiazole (P2b-Bz)



<i>Reagents/Solvents</i>	<i>Molar ratio</i>	<i>Numbers of moles (mmol)</i>	<i>Mw (g/mol)</i>	<i>Quantity</i>
2b	1.0	0.17	600.04	0.100 g
Bz	1.0	0.17	388.10	0.065 g
NaHCO_3	5.0	0.85	84.00	0.072 g
Pd(dppf)Cl_2	0.1	0.02	816.00	0.014 g
THF				4.0 mL
H_2O				2.0 mL

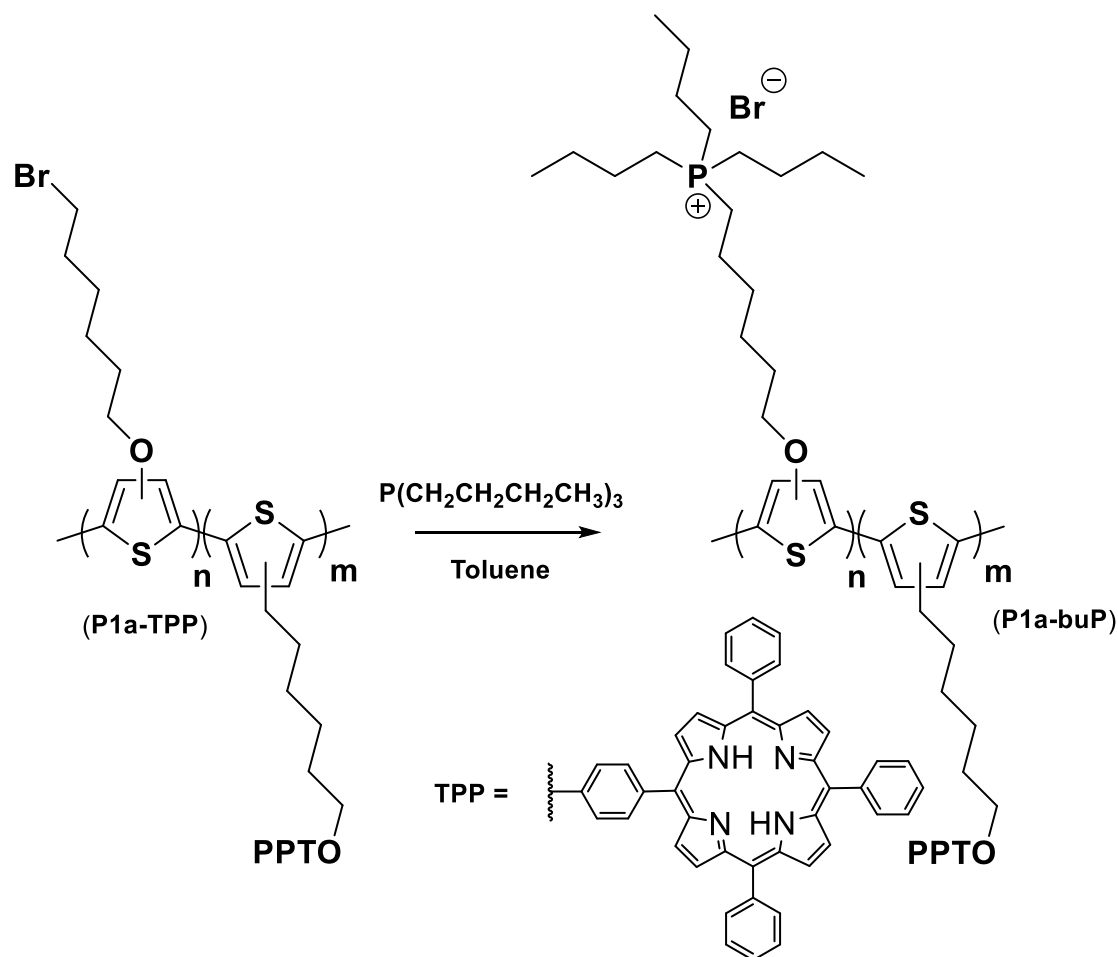
The same procedure described for P1b-Bz was followed starting from 2b (0.100 g, 0.17 mmol), Bz (0.065 g, 0.17 mmol) and Pd(dppf)Cl_2 (0.014 g, 0.02 mmol), to obtain 0.050 g of poly4-[3,4-(6,6'-dibromohexyloxy)thiophen-2-yl]benzo[c][1,2,5]thiadiazole (**P2b-Bz**) as sticky bordeaux solid (50% yield).

δ ^1H (400 MHz, CDCl_3 , ppm): 8.72-8.21 (br m, terminal Bz-H), 7.78-7.33 (br m, Bz-H and terminal Th-H), 4.17 (br t, ThOCH_2), 3.39 (br t, CH_2Br), 2.04-0.98 (br m, $(\text{CH}_2)_n$).

FT-IR (KBr, cm^{-1}): 2919, 2850, 1537, 1494, 1463, 1343, 1261, 1167, 1097, 1026, 801, 645, 562, 526.

Synthesis of ionic polymers: post-functionalization reaction with PBu_3

Poly{3-(6-tributylphosphoniumhexyloxy)thiophene-co-3-[5-(4-phenoxy)-10,15,20-triphenylporphyrinyl]hexylthiophene bromide} (**P1a-buP**)



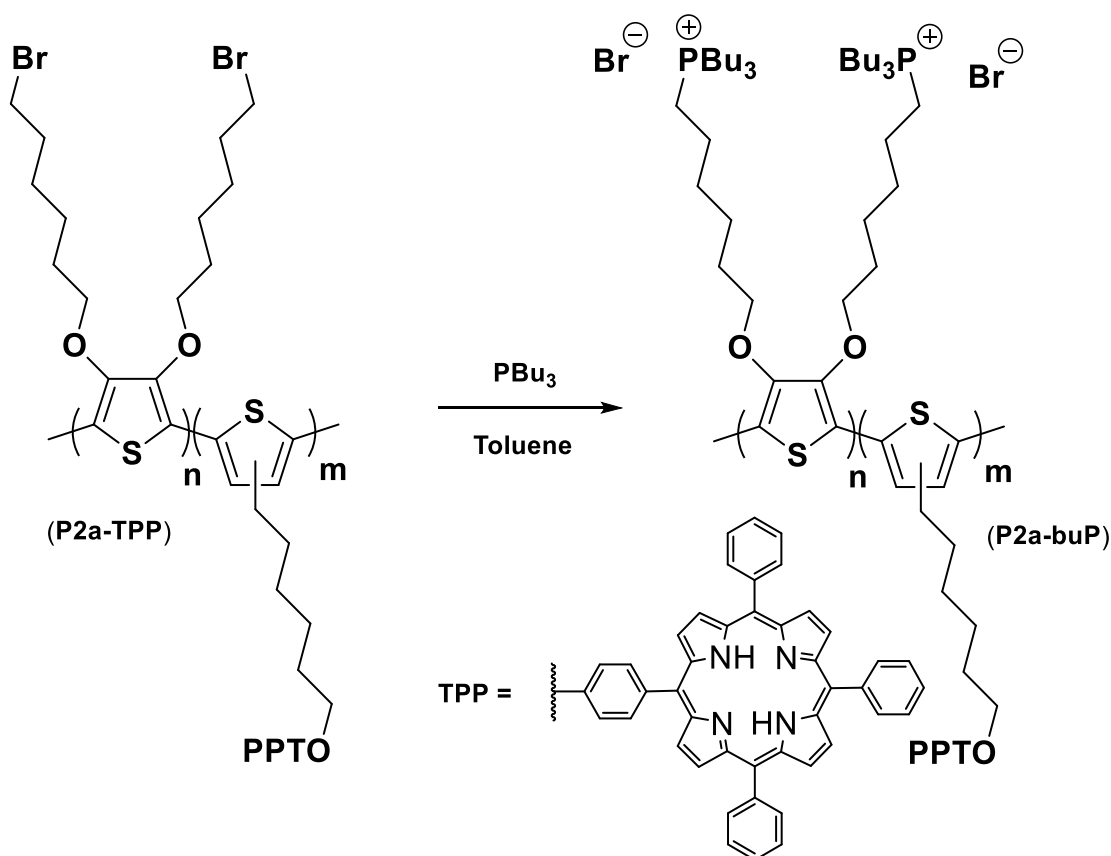
Reagents/Solvents	Molar ratio	Numbers of moles (mmol)	Mw (g/mol)	Quantity
P1a-TPP	1.0	0.27	373.28	0.100 g
PBu_3	10.0	2.72	203.00	0.7 mL
Toluene				10.0 mL

In a three-necked flask, after solubilizing the precursor polymer (**P1a-TPP**) in toluene, tributyl phosphine (PBu_3) was added to the system under nitrogen flow. The mixture was left to react for 24h under stirring at 90°C . Once the indicated time ran out, the supernatant was removed and the polyelectrolyte filmed on the flask surface was washed with Et_2O and recovered with MeOH. After drying under vacuum, 0.112 g (78% yield) of poly{3-(6-tributylphosphoniumhexyloxy)thiophene-co-3-[5-(4-phenoxy)-10,15,20-triphenylporphyrinyl]hexylthiophene bromide} (**P1a-buP**) as brown/purple solid was obtained.

δ ^1H (400 MHz, CD_3OD , ppm): 8.84 (br m, 8H, Pyrrolic-H), 8.21 (br m, 4H, Ar-H), 8.02 (br m, 4H, Ar-H), 7.83 and 7.72 (br m, 9H, Ar-H), 7.20-6.90 (br m, 4H, Ar-H and Th-H), 4.61 (br s, 2H, NH), 4.26 (br t, 2H, CH_2OTPP), 4.18 (br t, 2H, ThOCH_2), 2.98 (br m, 2H, ThCH_2), 2.21 (br s, 8H, $\text{CH}_2\text{P}^+\text{CH}_2$), 1.95 and 1.54 (br m, $(\text{CH}_2)_n$), 0.93 (br s, 9H, CH_3).

FT-IR (KBr, cm^{-1}): 3388, 2930, 2870, 1605, 1513, 1464, 1350, 1244, 1174, 1071, 1001, 965, 910, 800, 732, 701, 646, 526.

Poly{3,4-(6,6'-tributylphosphoniumdihexyloxy)thiophene-co-3-[5-(4-phenoxy)-10,15,20-triphenylporphyrinyl]hexylthiophene bromide} (**P2a-buP**)



Reagents/Solvents	Molar ratio	Numbers of moles (mmol)	Mw (g/mol)	Quantity
P2a-TPP	1.0	0.23	530.44	0.120 g
PBu ₃	20.0	4.50	203.00	1.3 mL
Toluene				10.0 mL

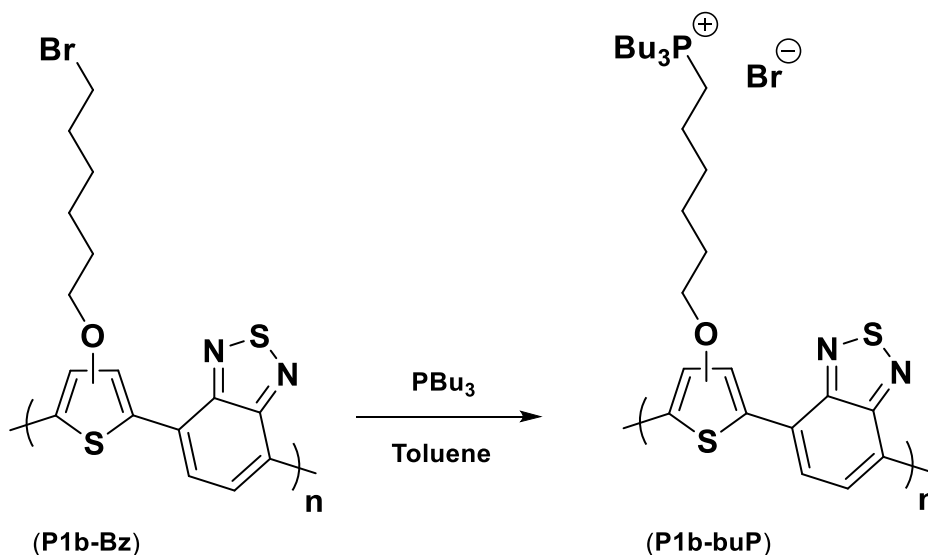
The same procedure described for P1a-buP was followed starting from P2a-TPP (0.120 g, 0.22 mmol) and PBu₃ (1.3 mL, 4.50 mmol), to obtain 0.135 g (89% yield) of poly{3,4-(6,6'-

tributylphosphoniumhexyloxy)thiophene-co-3-[5-(4-phenoxy)-10,15,20-triphenylporphyrinyl]hexylthiophene bromide} (**P2a-buP**), which appears as a bordeaux solid.

δ ^1H (400 MHz, CD_3OD , ppm): 8.82 (br m, 8H, Pyrrolic-H), 8.19 (br m, 8H, Ar-H), 7.83 (br m, 9H, Ar-H), 7.50-7.25 (br m, 2H, Ar-H), 6.98 (br m, 1H, Th-H), 4.57 (br s, 2H, NH), 4.20 (br m, 4H, CH_2OTPP and ThOCH_2), 2.80 (br m, 2H, ThCH_2), 2.27 (br s, 8H, $\text{CH}_2\text{P}^+\text{CH}_2$), 1.98 and 1.56 (br m, $(\text{CH}_2)_n$), 0.99 (br s, 9H, CH_3).

FT-IR (KBr, cm^{-1}): 3416, 2958, 2933, 2872, 1621, 1464, 1379, 1099, 916 839 750, 646, 526.

Poly4-[3-(6-tributylphosphoniumhexyloxy)thiophen-2-yl]benzo[c][1,2,5]thiadiazole (**P1b-buP**)



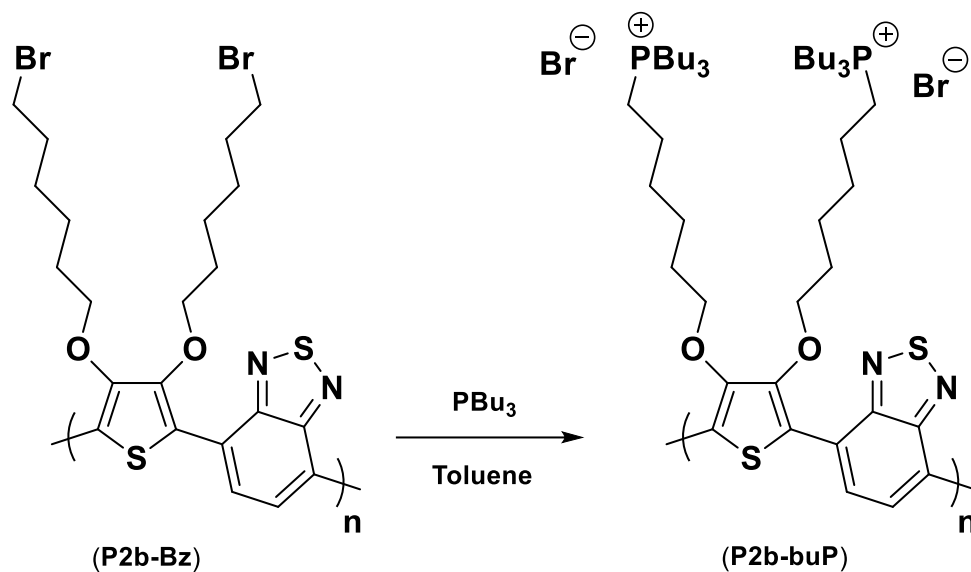
Reagents/Solvents	Molar ratio	Numbers of moles (mmol)	Mw (g/mol)	Quantity
P1b-Bz	1.0	0.18	395.35	0.079 g
P Bu ₃	10.0	1.80	203.00	0.5 mL
Toluene				12.0 mL

The same procedure described for P1a-buP was followed starting from P1b-Bz (0.079 g, 0.18 mmol) and P Bu₃ (0.5 mL, 1.80 mmol), to obtain 0.077 g (72% yield) of poly4-[3-(6-tributylphosphoniumhexyloxy)thiophen-2-yl]benzo[c][1,2,5]thiadiazole (**P1b-buP**), which appears as a blue solid.

δ ^1H (400 MHz, CD_3OD , ppm): 8.32-6.70 (br m, Bz-H and Th-H), 4.03 (br m, ThOCH_2), 2.20 (br m, $\text{CH}_2\text{P}^+\text{CH}_2$), 1.74 and 1.52 (br m, $(\text{CH}_2)_n$), 0.97 (br t, CH_3).

FT-IR (KBr, cm^{-1}): 3400, 2931, 2871, 1540, 1484, 1464, 1418, 1380, 1174, 1095, 832, 749, 646, 609

Poly4-[3,4-(6'6-tributylphosphoniumdihexyloxy)thiophen-2-yl]benzo[c][1,2,5]thiadiazole (**P2b-buP**)



Reagents/Solvents	Molar ratio	Numbers of moles (mmol)	Mw (g/mol)	Quantity
P2b-Bz	1.0	0.09	574.00	0.050 g
PBU ₃	20.0	1.74	203.44	0.5 mL
Toluene				5.0 mL

The same procedure described for P1a-buP was followed starting from P2b-Bz (0.050 g, 0.09 mmol) and PBU₃ (0.5 mL 1,74 mmol), to obtain 0.035 g (50% yield) of poly4-[3,4-(6'6-tributylphosphoniumdihexyloxy)thiophen-2-yl]benzo[c][1,2,5]thiadiazole (**P2b-buP**), which appears as a dark red solid.

δ ¹H (400 MHz, CD₃OD, ppm): 8.80-8.16 e 8.06-7.08 (br m, Bz-H and Th-H), 4.22 (br t, ThOCH₂), 2.78-1.95 (br m, CH₂P⁺CH₂), 1.95-1.15 (br m, (CH₂)_n), 1.15-0.38 (br t, CH₃).

FT-IR (KBr, cm⁻¹): 3401, 2957, 2932, 2871, 1733, 1624, 1542, 1492, 1463, 1379, 1230, 1097, 1050, 909, 837, 751.

4. Organic solar cells

The device substrates consist of small square slides (2 x 2 cm) on which a thin layer of a mixture of In_2O_3 and SnO_2 (ITO) is deposited. The anode was made by etching with a 10% wt. aqueous solution of HCl, at 60 °C for 15 minutes, in order to obtain an area of 1.5 x 1.0 cm covered by ITO. The substrates were then washed with distilled water, isopropyl alcohol and dried with nitrogen flow. A solution of poly(3,4-ethylenedioxythiophene):polystyrene sulfonic acid (PEDOT:PSS) in water was diluted 1:1 with isopropyl alcohol and then allowed to sonicate for 30 min. Covering 5.0 mm of ITO with adhesive tape, the solution was deposited on the previously etched glass substrates by using DoctorBlade technique. Let to air dry, the slides were heated in a glass oven under vacuum at 120°C for 90 minutes. On the still-warm substrates, a solution made by mixing 2.5 mg of PT6buP and 2.5 mg of C_{60} -Ser in 0.5 mL of EtOH as active layer was deposited by using DoctorBlade technique. Once the solvent was evaporated, a second thermal annealing was carried out at 120°C for 30 minutes. Then, before the cathode deposition, 1.0 mL of a solution of synthesized ionic materials (**P0a-b**, **P1a-b**, **P2a-b**) in EtOH (2 mg/mL) as interlayer was also deposited by spray-coating and subsequently annealed at 120°C for 30 min. The cathode, which consists of a nanometer layer of aluminum, was finally deposited by an high vacuum instrument (at about 10^{-6} mbar) through sublimation of a small amount of aluminum deposited on a tungsten filament where an intense current flows. Once the metallation was completed, the photovoltaic cells were measured using an instrument that provides illumination similar to solar radiation (solar-simulator).

References

1. Oil demand to peak in three years, says energy adviser DNV GL. *Reuters*. <https://www.reuters.com/article/us-oil-demand-dnv-gl-idUSKCN1VV2UQ>. Published September 10, 2019.
2. Schiermeier Q, Tollefson J, Scully T, Witze A, Morton O. Energy alternatives: Electricity without carbon. *Nature*. 2008;454(7206):816-823. doi:10.1038/454816a
3. Sovacool BK. National context drives concerns. *Nat Energy*. 2018;3(10):820-821. doi:10.1038/s41560-018-0246-5
4. Razykov TM, Ferekides CS, Morel D, Stefanakos E, Ullal HS, Upadhyaya HM. Solar photovoltaic electricity: Current status and future prospects. *Solar Energy*. 2011;85(8):1580-1608. doi:10.1016/j.solener.2010.12.002
5. What is coal & where is it found? World Coal Association. Accessed January 31, 2023. <https://www.worldcoal.org/coal-facts/what-is-coal-where-is-it-found/>
6. O.K S, Nair P, Ashok A. Chapter 41-Engineered nanomaterials for energy applications- "Nanomaterials for Solar Energy Generation". In ; 2018:751-767.
7. Mercadillo VO, Chan KC, Caironi M, Athanassiou A, Bissett M, Cataldi P. Electrically Conductive 2D Material Coatings for Flexible & Stretchable Electronics: A Comparative Review of Graphenes & MXenes.
8. Skotheim TA. *Handbook of Conducting Polymers, Second Edition*,. CRC Press; 1997.
9. Kawashima H, Kawabata K, Wang A, Goto H. Synthesis and optical properties of poly(phenylenethiophene)s bearing conjugated side chains. *Designed Monomers and Polymers*. 2015;18:661-668. doi:10.1080/15685551.2015.1070498
10. Zhang W. *Metal Halide Perovskite Crystals: Growth Techniques, Properties and Emerging Applications*. MDPI; 2019.

11. Polymers | Chemistry and Physics of Modern Materials, Third Edition
<https://www.taylorfrancis.com/books/mono/10.1201/9781420009873/polymers-valeria-arrighi-cowie>
12. Design, synthesis, and control of conducting polymer architectures: structurally homogeneous poly(3-alkylthiophenes) | The Journal of Organic Chemistry.
<https://pubs.acs.org/doi/10.1021/jo00056a024>
13. Novel, Highly Conducting, and Soluble Polymers from Anodic Coupling of Alkyl-Substituted Cyclopentadithiophene Monomers
Macromolecules.<https://pubs.acs.org/doi/10.1021/ma00085a043>
14. McCullough RD, Lowe RD. Enhanced electrical conductivity in regioselectively synthesized poly(3-alkylthiophenes). *J Chem Soc, Chem Commun.* 1992;(1):70-72.
doi:10.1039/C39920000070
15. Mehmood U, Al-Ahmed A, Hussein IA. Review on recent advances in polythiophene based photovoltaic devices. *Renewable and Sustainable Energy Reviews.* 2016;57(C):550-561.
16. Molecules | Free Full-Text | Thiophene-Based Covalent Organic Frameworks: Synthesis, Photophysics and Light-Driven Applications.2023. <https://www.mdpi.com/1420-3049/26/24/7666>
17. Hoppe H, Sariciftci NS. Organic solar cells: An overview. *Journal of Materials Research.* 2004;19(7):1924-1945. doi:10.1557/JMR.2004.0252
18. Polo E. *Caratterizzazione di materiali polimerici. Tecniche per polimeri fusi e allo stato solido.* Edizioni Nuova Cultura; 2016.
19. Classroom experiments and teaching materials on OLEDs with semiconducting polymers.
https://www.scielo.org.mx/scielo.php?pid=S0187-893X2013000100004&script=sci_arttext&tlng=en
20. Sun SS, Dalton LR, eds. *Introduction to Organic Electronic and Optoelectronic Materials and Devices.* 2nd ed. CRC Press; 2016. doi:10.1201/9781315374185
21. Advances in Molecular Design and Synthesis of Regioregular Polythiophenes | Accounts of Chemical Research. 2023. <https://pubs.acs.org/doi/full/10.1021/ar800130s>

22. Hou W, Xiao Y, Han G, Lin JY. The Applications of Polymers in Solar Cells: A Review. *Polymers*. 2019;11(1):143. doi:10.3390/polym11010143
23. Nayak PK, Mahesh S, Snaith HJ, Cahen D. Photovoltaic solar cell technologies: analysing the state of the art. *Nat Rev Mater*. 2019;4(4):269-285. doi:10.1038/s41578-019-0097-0
24. Rational Design of High Performance Conjugated Polymers for Organic Solar Cells | *Macromolecules*. 2023. <https://pubs.acs.org/doi/10.1021/ma201648t>
25. The future of organic photovoltaics - Chemical Society Reviews (RSC Publishing) DOI:10.1039/C4CS00227J. <https://pubs.rsc.org/en/content/articlehtml/2014/cs/c4cs00227j>
26. Conjugated Polymer-Based Organic Solar Cells | *Chemical Reviews*. Accessed March 1, 2023. <https://pubs.acs.org/doi/full/10.1021/cr050149z>
27. Molecular Bulk Heterojunctions: An Emerging Approach to Organic Solar Cells | *Accounts of Chemical Research* <https://pubs.acs.org/doi/10.1021/ar900041b>
28. Po R, Roncali J. Beyond efficiency: scalability of molecular donor materials for organic photovoltaics. *Journal of Materials Chemistry C*. 2016;4(17):3677-3685. doi:10.1039/C5TC03740A
29. Hossain MdA, Khoo KT, Cui X, et al. Atomic layer deposition enabling higher efficiency solar cells: A review. *Nano Materials Science*. 2020;2(3):204-226. doi:10.1016/j.nanoms.2019.10.001
30. Firdaus Y, Maffei LP, Cruciani F, et al. Polymer Main-Chain Substitution Effects on the Efficiency of Nonfullerene BHJ Solar Cells. *Advanced Energy Materials*. 2017;7(21):1700834. doi:10.1002/aenm.201700834
31. Ratcliff EL, Zacher B, Armstrong NR. Selective Interlayers and Contacts in Organic Photovoltaic Cells. *J Phys Chem Lett*. 2011;2(11):1337-1350. doi:10.1021/jz2002259
32. Lai TH, Tsang SW, Manders JR, Chen S, So F. Properties of interlayer for organic photovoltaics. *Materials Today*. 2013;16(11):424-432. doi:10.1016/j.mattod.2013.10.001
33. Dupont J. 2,1,3-Benzothiadiazole and Derivatives: Synthesis, Properties, Reactions, and Applications in Light Technology of Small Molecules. *European Journal of Organic Chemistry*. Published online January 1, 2013.

https://www.academia.edu/38992609/2_1_3_Benzothiadiazole_and_Derivatives_Synthesis_Properties_Reactions_and_Applications_in_Light_Technology_of_Small_Molecules

34. Lanzi M, Quadretti D, Marinelli M, Ziai Y, Salatelli E, Pierini F. Influence of the Active Layer Structure on the Photovoltaic Performance of Water-Soluble Polythiophene-Based Solar Cells. *Polymers*. 2021;13(10):1640. doi:10.3390/polym13101640